The Abdus Salam
International Centre for Theoretical Physics

United Nations
Educational, Scientific and
Cultural Organization

IAEA
International Atomic Energy Agency

2060-47

Advanced School on Non-linear Dynamics and Earthquake Prediction

28 September - 10 October, 2009

Application of the Block Structure Modeling to Study Relation between Geodynamics and Seismicity

I. Vorobieva
International Institute of Earthquake Prediction Theory and Mathematical Geophysics
Moscow
Russia

Pure appl. geophys. 164 (2007) 2193–2234
0033–4553/07/112193–42
DOI 10.1007/s00024-007-0273-9

Pure and Applied Geophysics

Simulation of Seismicity in the Block-structure Model of Italy and its Surroundings

A. Peresan,[1] I. Vorobieva,[2] A. Soloviev,[2,3] and G. F. Panza[1,3]

Abstract—The numerical block-model of the lithosphere dynamics is used to simulate seismicity in Italy and its surroundings, based on the available structural and geodynamics information. The purpose of the study is to understand which are the tectonic processes that control the main features of the observed seismicity and the kinematics of the region. The influence of the rheology of the fault systems is studied as well. The model we use differs from other modeling approaches in that it simulates earthquakes and hence it possibly relates to seismicity and geodynamics. The model provides an effective capability to include the set of documented constraints supplied by widely available earthquake catalogs. This is done by means of the comparison of the GR relation, of the focal mechanisms and of the space distribution for observed and computed seismicity. The region is modeled as a system of perfectly rigid blocks, separated by infinitely thin fault planes, in viscoelastic interaction between themselves and with the underlying medium. The movement of the boundary blocks and of the underlying medium determines the motion of the blocks. The synthetic seismicity obtained with the defined block-model is similar to the observed one for the most seismically active areas. A linear frequency-magnitude (FM) relation (Gutenberg-Richter law) is obtained for synthetic earthquakes; the slope (b-value) of the FM plot appears larger for the synthetic seismicity than for the observed one. Nevertheless, the b-value is essentially larger in northern and central Italy than that in southern Italy, both in the model and in the observations. The analysis of the source mechanisms of the synthetic earthquakes shows a good agreement with the observations. In the model normal faulting is typical for the Apennines, the eastern edge of Sicily and the Calabrian arc, while reverse faulting takes place at the northwestern boundary of the Adriatic Sea, in the southern Alps and along the eastern edge of the Adria, along the Dinarides. The model correctly reproduces the extension zone along the Apennines and the contraction zone along the northwestern boundary of the Adriatic Sea; the counter-clockwise rotation of the Adria is mimed. The resulting movements of the blocks are in overall agreement with GPS (Global Positioning System) observations. The results of the modeling experiments suggest that the main features of dynamics and seismicity in the central Mediterranean region cannot be satisfactorily explained as a consequence of Africa and Eurasia convergence only; the passive subduction in the Calabrian arc and the different rheology of faults are essential as well.

Key words: Block-model, numerical simulation, seismicity, synthetic catalog, lithosphere dynamics, Italy.

[1] Department of Earth Sciences, University of Trieste, via E. Weiss 1, 34127 Trieste, Italy.
E-mail: aperesan@units.it

[2] International Institute of Earthquake Prediction Theory and Mathematical Geophysics, Russian Academy of Sciences, Profsoyuznaya str. 84/32, 117997 Moscow, Russia.

[3] The Abdus Salam International Centre for Theoretical Physics - ESP, ICTP, 34100 Trieste, Miramare, Italy.

1. Introduction

Earthquakes occur as a result of different processes that are still not entirely described and understood. In the study of seismicity, a possible approach to overcome the difficulties which are caused by the absence of fundamental constitutive equations for the dynamics of the lithosphere and by the impossibility of direct measurements at depth, where the earthquakes originate, relies on the integration of the numerical modeling of the lithosphere dynamics with the phenomenology of earthquake occurrence.

A number of dynamical models have been proposed to simulate seismicity, the most popular being the spring-slider block-model of BURRIDGE and KNOPOFF (1967). Some models are "non-Earth specific" and reproduce only the very general features of seismicity, such as the frequency-magnitude relation. Others try to simulate, at the cost of additional assumptions, further properties of the seismic sequences, such as fluctuations in the activity and the space distribution of events (e.g., YAMASHITA and KNOPOFF, 1992). Each model tries to reproduce some peculiar properties of seismicity, based on different dynamical, kinematical or geometrical assumptions; nevertheless, no model can be expected to describe exactly the evolution of the Earth system, due to its complexity and possibly chaotic behavior.

Another type of numerical models that have been proposed so far is focused on the study of geodynamics. Among the studies devoted to the Mediterranean region, we recall the thin-sheet viscous model (BASSI and SABADINI, 1994; BASSI *et al.*, 1997; NEGREDO *et al.*, 1999), which is providing insights on the subduction zone underneath the Calabrian arc, and the two-dimensional elastic thin-shell modeling (MEIJER and WORTEL, 1996; LUNDGREN *et al.*, 1998), which was applied to study the kinematics and stress patterns in the Aegean region (GIUNCHI *et al.*, 1996). Recently, JIMENEZ-MUNT *et al.* (2003) used the thin-shell finite-element approach to simulate active deformation in the Mediterranean region. Finally, BATTAGLIA *et al.* (2004) used GPS data and the model proposed by MURRAY and SEGALL (2001) to investigate present-day deformation of the Adriatic region. The modeling they use, which computes rigid-plate angular velocities while accounting for elastic strain accumulation along block-bounding faults, is basically different from the block-structure dynamics simulation introduced by GABRIELOV *et al.* (1990), that we use in this study (hereinafter simply referred as "block-model").

The numerical models mentioned above, with the exception of the block-model, permit study of the geodynamics of a region under consideration. Using such models one can predict velocities, slip rates, stresses and other physical parameters and try to reconstruct the geological history of the region; nevertheless they do not simulate earthquakes. The block model considered in this paper, instead, simulates both fast (synthetic seismicity) and slow (tectonic motions) movements of blocks, and thus permits to study seismicity and its connection with the geodynamics of a given region. This represents the main advantage of the considered model, since it provides an effective capability to include the set of documented constraints supplied by widely available earthquake catalogs. This is done by means of the comparison of the Gutenberg-Richter

relation, of the focal mechanisms and of the space distribution for observed and computed seismicity.

The block-model described in detail by SOLOVIEV and ISMAIL-ZADEH (2003) provides a straightforward tool for a broad range of problems, such as the study of the dependence of seismicity on the general properties of the fault networks and rheology and the formulation and testing of different hypotheses for earthquake forecasting purposes. This is made possible by the introduction of some simplifications, the basic one being the assumption that the blocks are perfectly rigid. This assumption is justified by the fact that in the lithosphere the effective elastic moduli of the fault zones are significantly smaller than the ones within the blocks and it is rather realistic for short (as compared with the geological history) periods of simulation (thousands of years). It might be argued that continental deformation should be described by a velocity field, rather than by the relative motions of rigid blocks. But a velocity field that describes the average deformation is only a partial description of what is happening, because it does not describe the detailed discontinuous deformation of the seismogenic layer (JACKSON, 2003). In the block-model the movement of blocks, which corresponds to a velocity field "discretized" at the scale of blocks, is reproduced as a result of modeling. The modeling approaches that consider the deformable elastic blocks, generally relevant for much longer periods of simulation (millions of years), may eventually provide input information for the present simulation, in order to test their compatibility with the features of observed seismicity.

The method allows us to use a representative geometry of the blocks, based on any relevant information. Driving tectonic forces (velocities of the boundary blocks and underlying medium) can be prescribed using geodetic data (GPS, VLBI), and the rheology of fault zones (parameters reflecting elasticity and viscosity) can be taken into account, as well, using the knowledge of the lithosphere structure, in terms of geometries and velocities of seismic waves propagation, and heat-flow data. The output of the modeling consists of kinematical data on the block movements that can be compared with observations (e.g., GPS), as well as of a synthetic earthquake catalog, where each event has origin time, coordinates of epicenter, magnitude and source mechanism. On the basis of the experience accumulated to date, the synthetic earthquake catalog reproduces not only some of the basic global features of observed seismicity like (a) the Gutenberg-Richter law (e.g., PANZA *et al.*, 1997), (b) the space and time clustering of earthquakes (MAKSIMOV and SOLOVIEV, 1999) and (c) the dependence of the occurrence of large earthquakes on the fragmentation of the faults network, and on the rotation of blocks (KEILIS-BOROK *et al.*, 1997), but also several regional features of seismicity, like (1) the epicenter distribution, (2) the relative level of seismic activity in different areas of the region and (3) the type of fault plane solution.

The geometry of real faults and blocks has been first considered in the block-model of the Vrancea (Romania) earthquake-prone region (PANZA *et al.*, 1997; SOLOVIEV *et al.*, 1999). The source mechanisms of the largest synthetic earthquakes resulted to be close to the average ones observed for the large earthquakes that occurred in the Vrancea subduction zone (SOLOVIEV *et al.*, 2000). The effect on the intermediate-depth seismicity

of a sinking relic slab beneath Vrancea has been studied, as well by means of the model of the block-structure dynamics (ISMAIL-ZADEH *et al.*, 1999). Changes in synthetic seismicity, due to small variations in the slab rotation, are in overall agreement with the hypothesis of PRESS and ALLEN (1995) that small changes in the direction of the plate motion control the pattern of seismic release.

The block-model of the Sunda arc has been used to study the dependence of synthetic seismicity features on the specified movements. SOLOVIEV and ISMAIL-ZADEH (2003) demonstrated that the main features of synthetic seismicity are close to observations when the movement of Australia relative to Eurasia is specified in accordance with HS2-NUVEL-1 model (GRIPP and GORDON, 1990). The block-model of the western Alps (VOROBIEVA *et al.*, 2000; SOLOVIEV and ISMAIL-ZADEH, 2003) has been developed on the basis of the morphostructural scheme due to CISTERNAS *et al.* (1985).

In this study we consider a region covering Italy and its surroundings. The purpose of the study is to understand which tectonic processes control the features of the observed seismicity and the kinematics of the region, as well as the influence of the rheology of the fault system on the seismicity. The block model has been outlined on the basis of the seismotectonic model developed by MELETTI *et al.* (2000) and of the space distribution of seismicity. The idea to represent this region as a system of perfectly rigid blocks is supported by the existence of some large, almost aseismic territories, like the Adria micro-plate. The area of active deformation along the Apennines, in the present study, is simplified: Apennines are represented by blocks bounded by a system of parallel faults, which are assumed to represent as a whole the complex system of small faults. To estimate the quality of the modeling, the results of the numerical simulation are compared with the observations. Specifically, the block motions are qualitatively checked against geodetic observations (GPS and VLBI), while the epicenter distribution, the location of the largest events, the type of source mechanisms and the slope of the Gutenberg-Richter law for the synthetic seismicity are compared with the observed ones.

2. *Description of the Model*

A block structure is a limited and simply connected part of a layer, d, with thickness H, bounded by two horizontal planes (Fig. 1). The portions of planes intersecting the layer, called "fault planes", form the lateral boundaries of the block structure and its subdivision into blocks. The intersection lines of the fault planes with the upper plane are called "the faults." The fault planes can have arbitrary dip angles, which are specified on the basis of information on the lithospheric structure of the region under consideration. A common point of two faults is called "vertex." The vertices on the upper and the lower planes are connected by a segment ("rib") of the intersection line of the corresponding fault planes (see Fig. 1). The upper and the lower surfaces of the blocks are polygons. The lower surface of the block is called "the bottom." The topology of the fault structures in the upper and lower planes is the same. The block structure is bordered by a

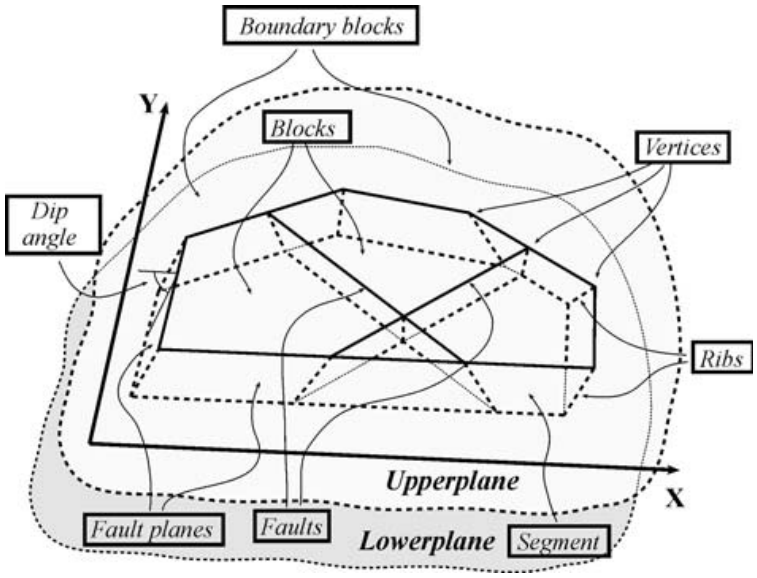

Figure 1
Definitions used in the block-structure model.

confining medium. The motion of the confining medium is defined in the continuous parts, delimited by two ribs of the block-structure boundary, called "boundary blocks." The blocks are assumed to be rigid, and their relative displacements take place along the fault planes. The interaction of the blocks with the underlying medium takes place along the lower plane, any kind of slip being possible. The fault planes and the bottoms of the blocks are assumed to be infinitely thin viscous-elastic layers.

The movements of the boundary blocks and of the underlying medium are assumed to be due to the external forces. The rates of these movements are assumed to be horizontal and known. The movement rates of the underlying medium and of the boundary blocks can be different for each block.

Dimensionless time is used in the model. All variables containing time are referred to one unit of the dimensionless time, and the real time corresponding to the unit of the dimensionless time can be estimated at the interpretation stage of the results.

Elastic forces arise in the lower plane and in the fault planes as a result of the displacement of the blocks relative to the underlying medium, to the lateral boundary, and to the other blocks. The elastic stress (the force per unit area) at a point is proportional to the difference between the relative displacement and the slippage (the inelastic displacement) at the point. The rate of the inelastic displacement is proportional to the elastic stress. Accordingly,

$$\mathbf{f} = K(\mathbf{\Delta r} - \delta\mathbf{r}), \quad \frac{d\delta r}{dt} = W\mathbf{f}, \tag{1}$$

where $\mathbf{f}$ is the shear stress vector (elastic force per unit area acting along the fault plane or the block base) at the point of the lower plane or of the fault plane, $\mathbf{\Delta r}$ is the vector representing the relative displacement, and $\delta\mathbf{r}$ is the vector representing the inelastic

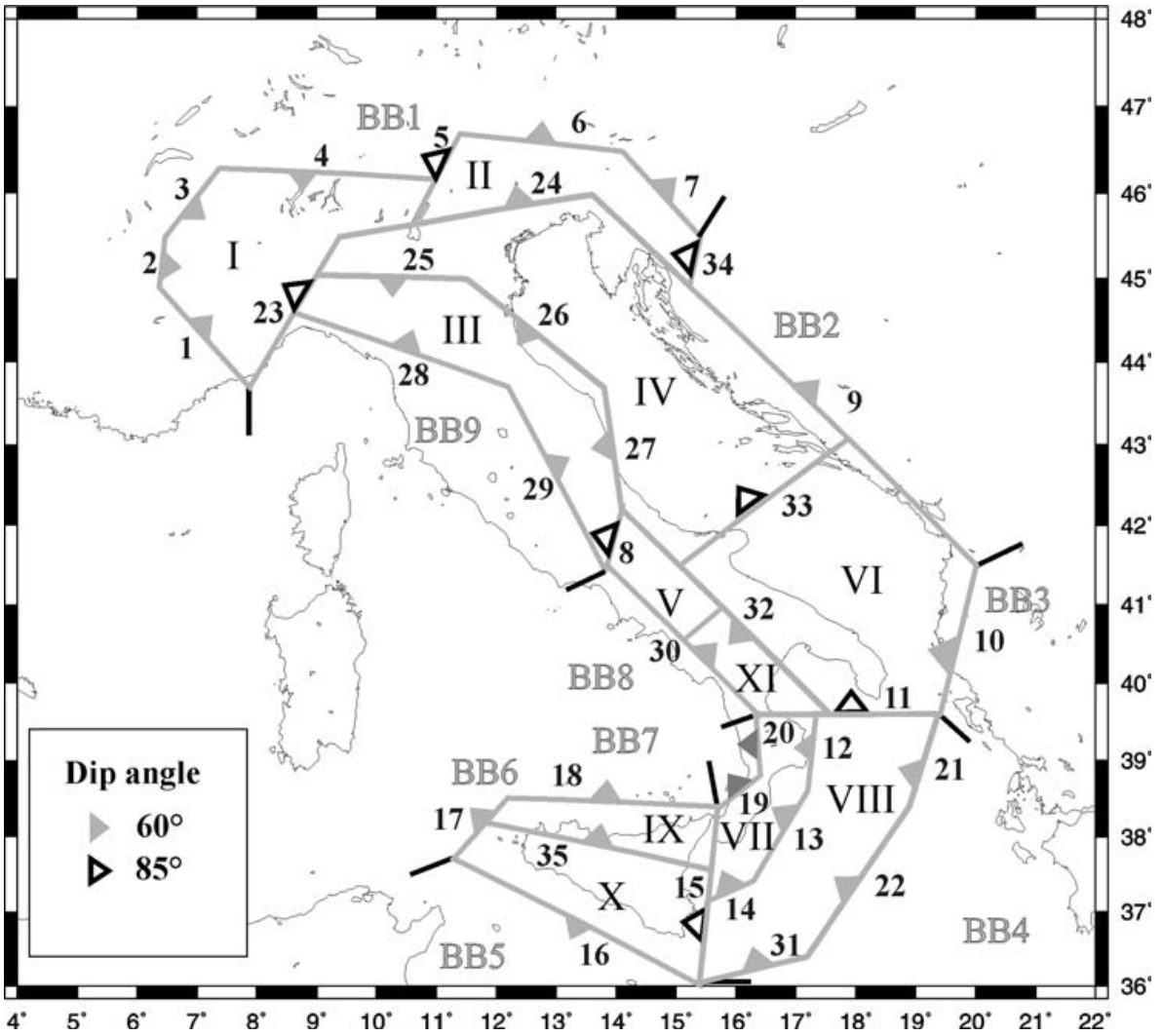

Figure 2
Geometry of the block-structure. I – XI – blocks; BB1– BB9 – boundary blocks.

displacement. Equations (1) correspond to visco elastic (Maxwell) rheological law that describes the relation of **f** to the strain $\boldsymbol{\zeta}$

$$\left(\frac{d}{dt}+\frac{1}{\tau}\right)\mathbf{f}=\mu\frac{d\zeta}{dt}, \tag{2}$$

where τ is the relaxation time ($\tau = \eta/\mu$), μ is the shear modulus, and η is the viscosity. Coefficients in (1) and (2) are connected by formulas: $K = \mu/a$, $W = a/\eta$, where a is the actual width of the fault zone and $\tau = 1/(KW)$.

On the fault plane, the reaction force is normal to the fault plane and its size, per unit area, is:

$$|p_0| = |f_1 \text{ tg } \alpha|, \tag{3}$$

where f_1 is the component of the elastic stress, **f**, normal to the fault on the upper plane, and α is the dip angle of the fault plane. The value of p_0 is positive in the case of extension and negative in the case of contraction, respectively.

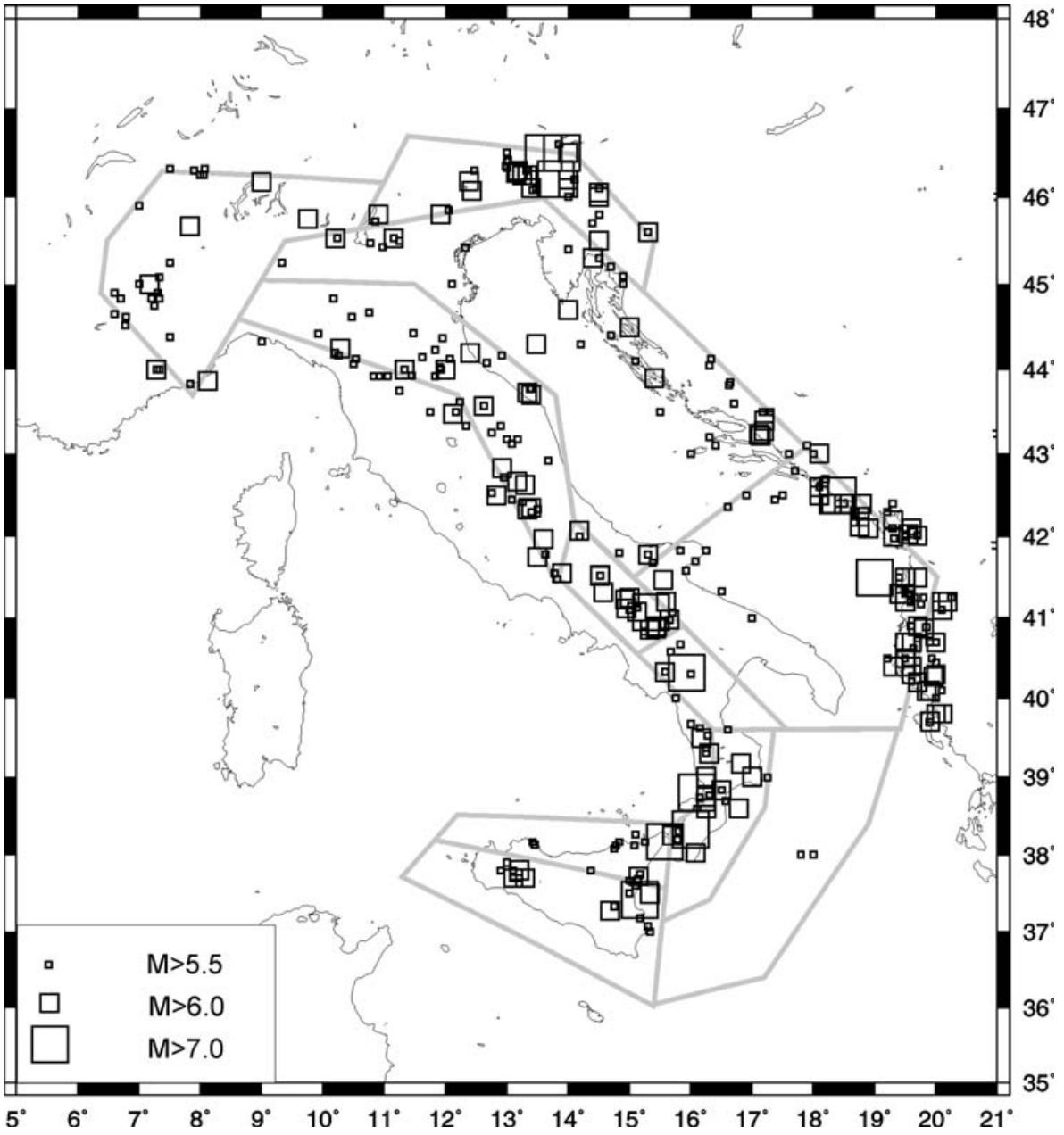

Figure 3
Observed seismicity with M ≥ 5.5, 1000–2000, (PERESAN and PANZA, 2002; LEYDECKER, 1991) and geometry of the block-structure.

The displacements of the blocks are described by the components of their translation vectors and the angles of their rotation around the geometrical centers and are presumed to be infinitely small, compared with the block size. Therefore the geometry of the block-structure does not change during the simulation and the structure does not move as a whole.

At each time moment the displacements of the blocks are found from the condition that the total force and the total moment of forces acting on each block are equal to zero. This is the condition of quasi-static equilibrium of the system and, at the same time, the condition of minimum energy. The equilibrium equations include only forces caused by

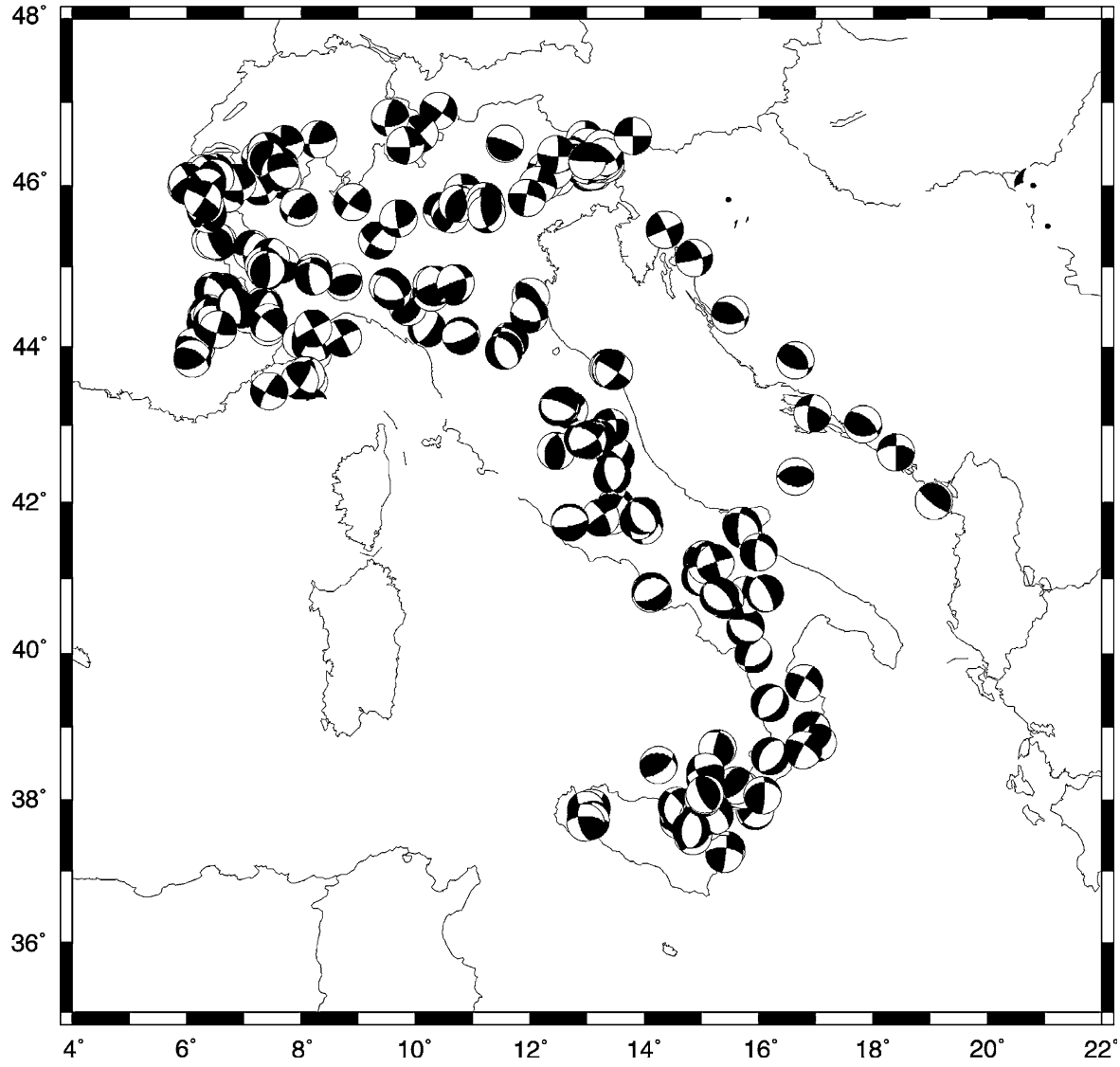

Figure 4
Observed fault plane solutions in the modeled region (SARAÒ *et al.*, 1997).

the specified movements of the underlying medium and the boundaries of the block-structure. In fact, it is assumed that the action of all other forces (gravity, etc.) on the block-structure is ruled out and does not cause displacements of blocks.

The state of the block-structure is considered at discrete values of time $t_i = t_0 + i\Delta t$ ($i = 1, 2, ...$), where t_0 is the initial time. The transition from the state at t_i to the state at t_{i+1} proceeds as follows: (i) new values of the inelastic displacements are calculated accordingly to equations (1); (ii) translation vectors and rotation angles at t_{i+1} are obtained for boundary blocks and the underlying medium; (iii) the translation vectors and the angles of rotation for the blocks are determined from the equilibrium equations.

The space discretization that is necessary to carry out the numerical simulation of block-structure dynamics is made by splitting the surfaces (fault planes and block

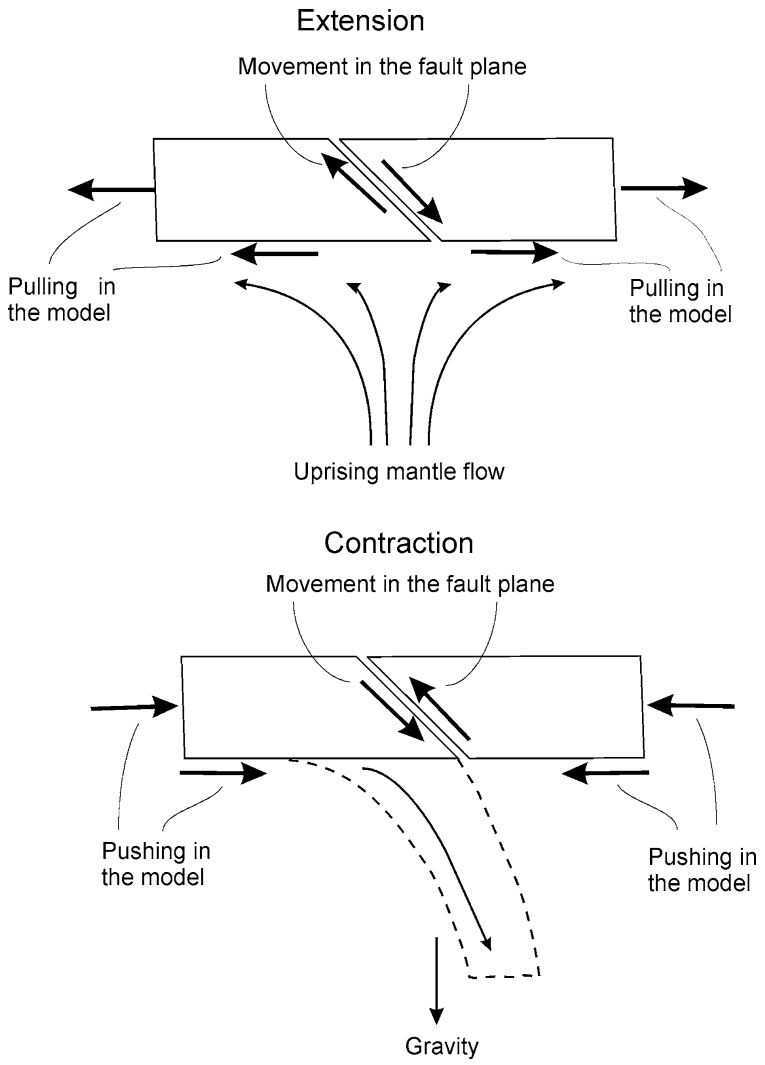

Figure 5
Scheme describing the modeling of non-horizontal movements (e.g., uprising mantle flow or gravity) in the two-dimensional model of the block-structure dynamics.

bottoms), on which the forces act, into cells with linear size not exceeding a parameter ε. The coordinates X, Y, the relative displacement $\mathbf{\Delta r}$, the inelastic displacement $\delta\mathbf{r}$, and the elastic stress $\mathbf{f}$ are assumed to be the same for all the points of a cell.

The earthquakes are simulated in accordance with the dry friction model. For each cell of the fault planes the quantity

$$\kappa = \frac{|\mathbf{f}|}{P - p_0} \tag{4}$$

is introduced, where $\mathbf{f}$ is given by (1), P is a parameter of the model which is assumed to be equal for all the faults. P can be interpreted as the difference between the lithostatic (due to gravity) and the hydrostatic pressure, which is assumed to be equal to 2 Kbars for all the faults, and p_0 is the reaction force per unit area, given by (3).
Three following values of κ are assigned for each fault:

$$B > H_f \geq H_s.$$

It is assumed that the initial conditions of the model satisfy the inequality $\kappa < B$ for all cells of the fault planes.

If, at some time t_i, the value of κ in any cell of a fault plane reaches the level B ($\kappa \geq B$), a failure ("earthquake") occurs. The failure is considered a slippage during which the inelastic displacement $\delta\mathbf{r}$ in this cell changes abruptly to reduce the value of κ to the level H_f. The new—after the failure—vector of the inelastic displacement $\delta\mathbf{r}^e$ is calculated from

$$\delta\mathbf{r}^e = \delta\mathbf{r} + \delta\mathbf{u}, \quad \delta\mathbf{u} = \gamma\mathbf{f}, \tag{5}$$

where $\delta\mathbf{r}$ and $\mathbf{f}$ are the inelastic displacement and the elastic stress, defined by (1), just before the failure and the coefficient γ is determined from the condition that $\kappa = H_f$ after the failure. Once the new values of the inelastic displacements for all the failed cells are computed, the translation vectors and the angles of rotation of the blocks are determined to satisfy the condition of quasi-static equilibrium. If after these computations, for some cell(s) of the fault planes still $\kappa > B$, the procedure is repeated for this (these) cell(s), otherwise the numerical simulation is continued in the standard way.

On the same fault plane, the cells in which failure simultaneously occurs form a single earthquake. The coordinates of the earthquake epicenter are determined as the weighted sum, with weights proportional to the areas of the failed cells, of the coordinates of the cells forming the earthquake. The magnitude of the earthquake is calculated from UTSU and SEKI, (1954)

$$M = 0.98 \ \log_{10} S + 3.93, \tag{6}$$

where S is the total area of the cells forming the earthquake, measured in km^2.

For each earthquake, the source mechanism can be determined considering the vector $\mathbf{\Delta U}$, defined as the weighted sum, with weights proportional to the areas of the failed cells, of the vectors $\delta\mathbf{u}$, given by (4), for the cells forming the earthquake. From (1) and (4) it follows that $\mathbf{\Delta U}$ lies in the fault plane where the earthquake occurs.

Immediately after each earthquake, it is assumed that the cells in which the failure occurred are in the creep state. It means that, for these cells, in equation (1), which describes the evolution of the inelastic displacement, the parameter W_s ($W_s > W$) is used instead of W. After the earthquake, the cell keeps in the creep state as long as $\kappa > H_s$, when $\kappa \leq H_s$, the cell returns to the normal state and henceforth the parameter W is used in (1) for this cell.

3. Geodynamics and Block Structure for the Italian Region and its Surroundings

Different criteria can be followed to define the geometry of the block structure which depends on the main geological elements of the region as well as the scale and detail of

the model. In some previous studies the morphostructural zonation of the study region, e.g., the western Alps (CISTERNAS *et al.*, 1985), has been used as the base for the block-structure geometry (VOROBIEVA *et al.*, 2000; SOLOVIEV and ISMAIL-ZADEH, 2003). In the present work, which is performed on a larger space dimension, we use as a base for the block-structure geometry the seismotectonic model of the study area (SCANDONE *et al.*, 1990, 1994; MELETTI *et al.*, 2000) and the space distribution of observed seismicity.

According to MELETTI *et al.* (1995, 2000), the recent geodynamics of the Central Mediterranean region is controlled by the Africa-Europe plate interaction and by the passive subduction of the south western margin of the Adria plate. The main regional geological features observed in Italy and surroundings are represented by the Alps, by the back arc Tyrrhenian extensional basin, by the Apennines and by the Padan-Adriatic-Ionic foreland. The Ortona-Roccamonfina line (SCANDONE *et al.*, 1990) connects two major arcs in the Apennines chain corresponding to the north-central and southern Apennines. The extensional rate that characterizes the southern part of the Tyrrhenian basin exceeds considerably those observed in the northern part; the boundary between these parts lies nearby at the 41°N parallel and it is associated with a discontinuity marked by magnetic anomalies.

Apennines, Alps and Dinarides outline the western, northern and eastern boundaries of the Adria respectively, while the location of the southern boundary is still controversial. A counter-clockwise rotation of the Adria seems to justify the main characteristics, both structural and kinematics, of its boundary regions (ANDERSON and JACKSON, 1987; WARD, 1994), such as the contraction front extending along the northeastern boundaries of the plate. Passing from east to west the structural features change: The Adria is subducting below the eastern Alps and the Apennines, while in the western Alps it is overthrusting the European plate (MELETTI *et al.*, 1995; SCHMID *et al.*, 1996). Hence the boundary between the Alps and the Apennines is a transform fault zone connecting the opposite lithospheric sinking. The evolution of the Apennines, however, does not seem to be explained by a simple convergence process and certain evidence suggests that it might be controlled by passive subduction processes (MELETTI *et al.*, 1995; PASQUALE *et al.*, 1997; DOGLIONI, 1991; DOGLIONI *et al.*, 1999a).

A band with tensional seismotectonic behavior, with prevailing dip-slip focal mechanism, characterizes the northern part of the Italian peninsula, from the Po plain to the Ortona-Roccamonfina line. Two belts run parallel to it: the western one is composed of the tensile zones near the Tyrrhenian coast and the eastern one by the contraction zones along the Adriatic Sea. The model proposed by MELETTI *et al.* (2000) for the deep structure of the north-central Apennines includes a connection at depth between the western Adriatic contraction front and the uplifting asthenosphere along the Tyrrhenian Sea. This agrees with the geometry of the lithosphere-asthenosphere system outlined by CALCAGNILE and PANZA (1981), PANZA *et al.* (1982), DELLA VEDOVA *et al.* (1991), MARSON *et al.* (1995) and refined by CHIMERA *et al.* (2003) and PANZA *et al.* (2003) on the basis of relevant geophysical observations (surface waves and body waves tomography, heat flow, gravity).

The subduction of the Adriatic foreland in the southern Apennines, from the Ortona-Roccamonfina line to the Taranto Gulf, seems to have ceased, while a passive subduction continues in the concave part of the Calabrian arc, where a zone of active seismicity is identified, emerging toward the Tyrrhenian basin and reaching a depth of about 500 km (CAPUTO *et al*., 1970, 1972; ANDERSON and JACKSON, 1987; PANZA *et al*., 2003).

Regarding the Adria plate, it still remains unclear if it is connected to the Africa plate or if it moves as an independent plate, since neither a structural nor a seismically active boundary between the Adria and Africa plate is clearly evidenced (PANZA, 1984). At the same time the movements of the Adria and Africa plates appear quite different: The stress distribution appears compatible with a counter-clockwise rotation of the Adria, with respect to Eurasia, with a rotation pole well distinguished from that proposed for the Africa-Eurasia rotation. The lithospheric heterogeneities recently outlined by VENISTI *et al*. (2005) seem to corroborate the hypothesis of fragmentation of the Adriatic plate, as required by the kinematics models of BENEDETTI (1999), the dynamic models of BATTAGLIA *et al*. (2004), and by the complex geodynamic evolution of the Balkan area (PAMIC *et al*., 2002).

Summing up, the available information is not sufficient to define the block structure of the region uniquely. The block structure we outlined for the dynamical modeling of seismicity in the Italian region is based on the main features of observed seismicity, and takes into account the geodynamic, structural and seismotectonic framework as proposed by MELETTI *et al*. (2000). The configuration of its faults, on the upper plane, is shown in Figure 2. Since one of the aims of the model is to reproduce the main features of the space distribution of observed seismicity (Fig. 3), the modeled faults have to be introduced in the structure corresponding to the most seismically active areas and fault zones. Together with the distribution of the observed seismicity, the outlined fault locations take into account the seismotectonic model of Italy (SCANDONE *et al*., 1994; MELETTI *et al*., 2000) as well.

The complex geodynamics of the studied region requires the use of an adequately complex block structure. Several parameters describing its dynamical properties must be defined for each block; hence the limited availability of observations pertaining to the real motion of the structure imposes limitations on the amount of details that can be introduced in the block structure (e.g. smallest block size).

The block structure (Fig. 2) consists of eleven blocks. These blocks are contoured by 36 faults. The point with the geographic coordinates 43.0°N and 13.0°E is chosen as the origin of the reference Cartesian coordinate system. The *X*-axis is the east-oriented parallel passing through the origin of the coordinate system and the *Y*-axis is the north-oriented meridian passing through the origin of the coordinate system. The blocks and the faults composing the structure are marked in Figure 2 by numerals from I to XI and from 1 to 36, respectively.

Since in the used block-model deformation is confined along fault planes, a double system of faults is defined to account for the tectonic belts where intense deformation takes place. Two main longitudinal discontinuities (faults 25–29) have been placed along

the north-central Apennines to model the Adriatic contraction front and the extension belt. Fault 8 has been placed corresponding to the Ortona-Roccamonfina line (MELETTI *et al*., 2000), while faults 30 and 32 have been placed south of it to model the seismic activity from Irpinia to the Pollino, along the southern Apennines. A possible discontinuity (fault 11) is assumed to exist between the Adria and Africa plates, south of Apulia; an almost EW-oriented discontinuity (fault 33) has been placed according to the observed seismicity, crossing the Gargano and the Adria plate from the Apenninic chain up to the Dinarides. BATTAGLIA *et al*. (2004) also assume a similar boundary, dividing Adria into two subplates separated by the Gargano-Dubrovnik fault, in agreement with the parametric studies by OLDOW *et al*. (2002). Nine boundary blocks, which are marked as BB1 - BB9 in Figure 2, are introduced to specify the motion of the confining medium at the lateral boundaries of the structure.

To choose the value of the thickness H of the layer d we analyze the distribution of the hypocenters of observed seismicity. Most of them are within 30-km depth. Another reason to specify $H = 30$ km is given by the recent data on the deep structure of Italy and surroundings. According to CHIMERA *et al*. (2003) and PANZA *et al*. (2003), there is a rather extended lithospheric region where, at an average depth of about 30 km, the S-wave velocity is rather low. This mantle wedge is a generalized feature, identified in the uppermost mantle along the Apennines and the Calabrian arc, and it underlies all the recent volcanoes. Therefore partial melting can be relevant in this part of the uppermost mantle, and it is reasonable to assume that this is a zone of increased plasticity, where lithospheric delamination occurs, with consequent decoupling between the upper and lower layers of the lithospheric mantle.

The dip angles of the faults have been specified on the basis of the source mechanisms of the observed earthquakes given in Figure 4 (SARAO' *et al*., 1997). The faults have been separated into two groups: near-vertical and oblique faults. The same value of the dip angle has been assigned to all the faults belonging to the same group: 85° for near-vertical faults, and 60° for oblique faults. The dip angle of each fault is indicated in Figure 2.

The results of recent geodynamical reconstructions for the central Mediterranean area have been considered for the numerical simulation, including GPS measurements (ANZIDEI *et al*., 1996; DEVOTI *et al*., 2002), VLBI (WARD, 1994) and paleomagnetic evidence (SAGNOTTI, 1992; SAGNOTTI *et al*., 1994; AIFA *et al*., 1988). The directions of the most compressive horizontal principal stress from the World Stress Map (MUELLER *et al*., 2000) and the map of active stress for the Italian region (MONTONE *et al*., 1999) have been taken into account as well. This information has been used to constrain the prescribed velocities of the boundary blocks and underlying medium.

A problem that we encounter in defining the model is the adequate representation, using a bidimensional system of absolutely rigid blocks, of the opening of the Tyrrhenian basin and of the passive subduction of the Ionian-Adria lithosphere, with the consequent flexure axis retreat. To reduce the problem to two dimensions we make the following assumption. The extension due to the uprising mantle flow is modeled by displacements

of blocks that can be obtained by means of a pulling force, applied by the boundary blocks and block bottoms (BUCK, 2003), while contraction can be described by means of a pushing force (see Fig. 5). This way we model non-horizontal driving forces and movements in the fault planes, applying equivalent horizontal driving motions. A similar task of reducing a three-dimensional problem to two dimensions has been considered by JIMENEZ-MUNT *et al*. (2003), where vertical forces have been reduced to their horizontal equivalents (e.g., trench suction in the Calabrian Arc).

The block structure thus defined and the above-mentioned information have been the starting point for a wide set of numerical experiments described below, which permitted, step by step, reproduction of several relevant features of the observed kinematics and seismicity.

4. Numerical Experiments

The values of the parameters for the blocks and the faults and the movements specified for the underlying medium and the boundary blocks have been varied in a set of parametric experiments. We report here about the six experiments that we consider most significant.

The following set of values has been assumed as a benchmark and we call it, from now on, the "standard set." The medium underlying all the blocks and the boundary blocks BB1–BB3 and BB6–BB9 does not move. The boundary blocks BB4 and BB5 move progressively with the velocity $V_x = -25$ cm, $V_y = 65$ cm per unit of dimensionless time, respectively. This direction of velocity has been chosen according to NUVEL-1A model (GRIPP and GORDON, 1990; DEMETS *et al*., 1990, 1994). For all blocks and faults the coefficients in (1) are: $K = 1$ bar/cm and $W = 0.05$ cm/bar. For all faults the thresholds for κ are: $B = 0.1$, $H_f = 0.085$, and $H_s = 0.07$, and for $W_s = 5$ cm/bar, like those used in previous studies (i.e., PANZA *et al*., 1997; SOLOVIEV *et al*., 2000; VOROBIEVA *et al*., 2000). These parameters reflect the rheology of fault zones in the dimensionless time domain considered for the modeling; a detailed analysis of these parameters and their relation with published estimations (see, e.g., KARNER *et al*., 2003) goes beyond the scope of the present study. In all experiments the value of P in (4) equals 2 Kbars, and the values of the parameters for the discretization, in time and space, are $\Delta t = 0.0001$ units and $\varepsilon = 5$ km, respectively.

In the first experiments we change step by step the movements of the underlying medium and of the boundary blocks taking into account the following main features of the geodynamics of the region:

- convergence of African and European plates;
- counterclockwise rotation of the Adria plate, with the pole of rotation in the western Alps;
- opening of the Tyrrhenian basin.

The influence of the rheology is studied in the final stage of study.

The following features of the observed seismicity, which follow from the analysis of the epicenter distribution and source mechanism, have been used to estimate the results of the experiments:

- two seismoactive belts in the north-central Apennines: The eastern one in contraction, the western one in extension;
- double extensional belt in the southern Apennines;
- contractional belts along the Dinarides and the southern Alps;
- absence of seismicity along the southern boundary of the structure, i.e., unknown boundary between Africa and Adria.

The number of free parameters in the model is rather high. They include six parameters (K, W, W_s, B, H_f, and H_s) for each of the thirty-six faults, five parameters (K, W, V_x, V_y, and the angular velocity) for each of the eleven block bottoms, three parameters (V_x, V_y, and the angular velocity) for each of the nine boundary blocks, and four general parameters (H, P, ε, and Δt). Nevertheless the parameters P, ε, Δt, K, B, H_f, and H_s are not changed in our numerical experiments and the prescribed angular velocity is set to zero for all block bottoms and boundary blocks. Moreover, when changing values of W and W_s the relation $W_s = 100\ W$ is preserved. This reduces the total number of free parameters, and actually, in the experiments described below, only a few of them were changed.

A qualitative comparison of the modeling results with observed seismicity and geodynamics is made in the first steps of the study (Experiments 1–5 below). The quantitative comparison is made in the final step (Experiment 6), for which a qualitative agreement with the observation is obtained.

4.1. Experiment 1

Purpose: To check whether the convergence of Africa and Europe alone can explain the main features of tectonics and seismicity in the region.

Values of the parameters: The standard set given above in this section.

Results: Adria undergoes a counterclockwise rotation, but its northern part (block IV) moves NW, and not northward, as it should be to reproduce observations (Nocquet and Calais, 2003). Most of the synthetic seismicity is concentrated along the southern boundary of the structure, where observed seismicity is absent. Excluding two clusters of events in the Alps, the synthetic seismicity is absent in the northern part of the model where, on the contrary, the observed seismicity is considerable. The average velocities of the blocks are listed in Table 1, and the epicenters of the synthetic earthquakes are shown in Figure 6.

4.2. Experiment 2

Purpose: To evaluate the dependence of the model behavior on the thickness of the structure.

Table 1

Experiment 1 (standard set)

Block	Prescribed velocities of underlying medium in cm per unit of dimensionless time		Average translational and angular velocities of blocks per unit of dimensionless time		
	V_x	V_y	V_x (cm)	V_y (cm)	ω (10^{-6} rad)
I	0	0	–1.30	–0.15	0.07
II	0	0	–0.20	0.33	–0.02
III	0	0	–1.14	0.13	0.10
IV	0	0	–3.33	4.59	0.26
V	0	0	1.22	0.58	0.00
VI	0	0	5.15	13.07	0.80
VII	0	0	–3.40	2.76	–0.12
VIII	0	0	–7.56	9.88	–0.04
IX	0	0	–3.02	2.54	–0.33
X	0	0	–9.51	8.77	–0.97
XI	0	0	4.03	2.98	0.46

Prescribed velocities of boundary blocks in cm per unit of dimensionless time

Boundary block	V_x	V_y
BB1–BB3, BB6–BB9	0	0
BB4	–25.00	65.00
BB5	–25.00	65.00

The prescribed angular velocity $\omega = 0$ for all boundary blocks and medium underlying blocks of structure in all experiments.

Values of the parameters: The standard set, except for the value of H, which is set to 15 km.

Results: The displacements of the blocks and the distribution of the epicenters of the synthetic earthquakes are similar to those obtained in Experiment 1, but the synthetic seismicity in the Alps disappears and the overall level of seismic activity decreases. The average velocities of the blocks are listed in Table 2, and the epicenters of the synthetic earthquakes are shown in Figure 7.

4.3. Experiment 3

Purpose: To reproduce the direction of motion of the northern part of the Adria (block IV), and to improve the fit with observed seismicity by removing the synthetic seismicity from the southern boundary of the block structure and by making its northern part seismically active.

Values of the parameters: The standard set is modified as follows. The translational velocities of the boundary block BB4 and of the underlying medium, for blocks IV–VIII and XI, correspond to a rotation of the Adria plate around the pole with geographical coordinates 44.2°N and 8.3°E (MELETTI *et al.*, 2000). This means that the prescribed

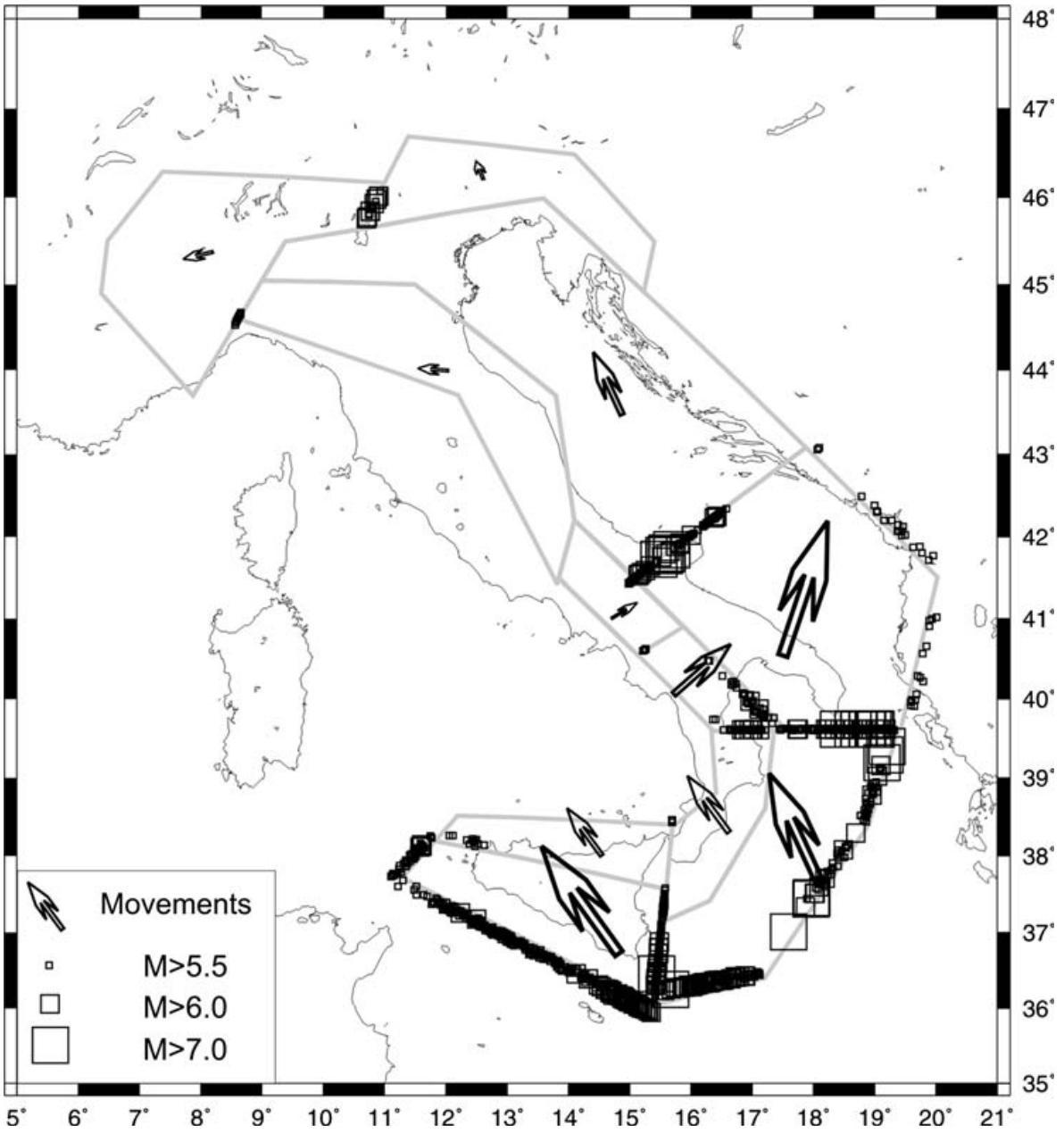

Figure 6
Synthetic seismicity and movements of block structure: Experiment 1.

velocities are orthogonal to the radius vector from the pole of rotation to the center of the block and that the values of the velocities are proportional to its distance from the pole of rotation (as given in Table 3). These NE-oriented velocities prescribed for the underlying medium account also for the possible global eastward drift of the asthenosphere relative to the lithosphere, as suggested by Doglioni *et al.* (1999b). No rotational components of velocity are prescribed. The velocity of the underlying medium for block X is the same as the velocity of the boundary block BB5, $V_x = -25$ cm, $V_y = 65$ cm per unit of dimensionless time.

Table 2

Experiment 2

Block	Prescribed velocities of underlying medium in cm per unit of dimensionless time		Average translational and angular velocities of blocks per unit of dimensionless time		
	V_x	V_y	V_x (cm)	V_y (cm)	ω (10^{-6} rad)
I	0	0	–0.34	–0.01	0.01
II	0	0	–0.12	0.10	–0.01
III	0	0	–0.33	–0.04	0.03
IV	0	0	–1.37	1.85	0.11
V	0	0	0.39	0.04	0.01
VI	0	0	1.63	5.72	0.38
VII	0	0	–1.58	2.00	–0.10
VIII	0	0	–4.35	5.20	–0.06
IX	0	0	–1.38	1.44	–0.27
X	0	0	–7.00	5.31	–0.81
XI	0	0	1.51	1.25	0.22

Prescribed velocities of boundary blocks in cm per unit of dimensionless time

Boundary block	V_x	V_y
BB1–BB3, BB6–BB9	0	0
BB4	–25.00	65.00
BB5	–25.00	65.00

Results: A counterclockwise rotational component of the movement for blocks IV and VI, representing the Adria plate, is obtained. The northern part of the Adria (block IV) moves northward. Extension along the double seismic belt in the southern Apennines (faults 30, 32) and contraction along the Dinarides (faults 9, 10) are obtained, although the model does not reproduce the extension–contraction belt in the north-central Apennines (faults 25–29). The southern boundary of the structure becomes aseismic, while the northern part of the structure is active upto the Alps. High seismicity appears at the eastern edge of Sicily. A seismic belt appears in the southern Apennines, however there is no synthetic seismicity at the western edge of the north-central Apennines. The level of seismicity is not high enough in the Calabrian arc and in the Dinarides. The average velocities of the blocks are listed in Table 3 and the epicenters of the synthetic earthquakes are shown in Figure 8.

4.4. Experiment 4

Purpose: To reproduce the extension–contraction belt in the North-Central Apennines and to increase the level of seismic activity in the Calabrian arc.

Values of the parameters: With respect to the set of parameters considered in Experiment 3, the following changes are made: The velocities of the boundary block BB7 and of the underlying medium for block III are replaced respectively by $V_x = -30$ cm, $V_y = 30$ cm, and by $V_x = 55$ cm, $V_y = 45$ cm per unit of dimensionless time.

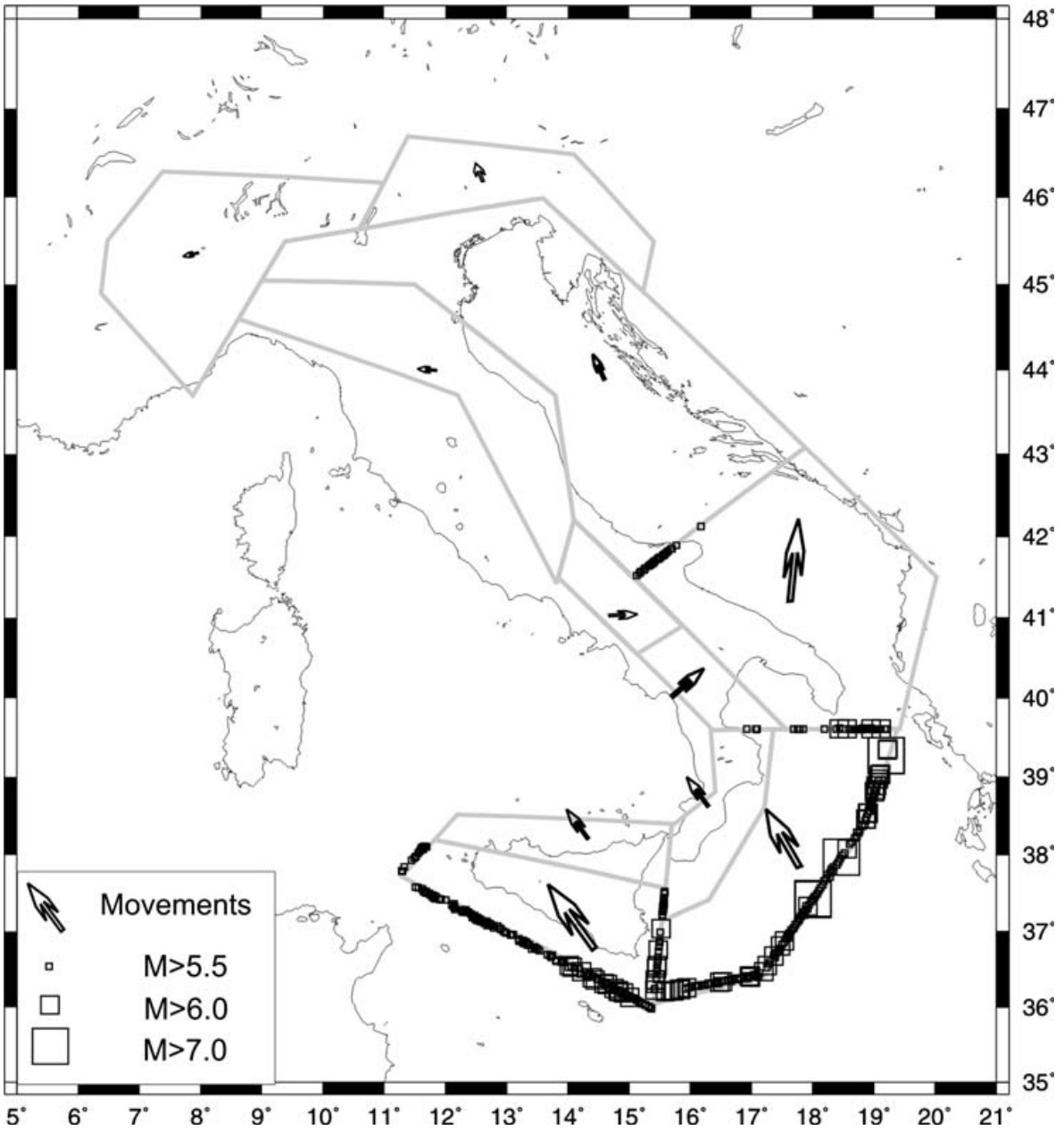

Figure 7
Synthetic seismicity and movements of block structure: Experiment 2.

Results: The counterclockwise rotation of the Adria plate, the extension in the southern Apennines and the contraction along the Dinarides are mimed. The extension–contraction belts in the north-central Apennines are obtained as well. A high synthetic seismic activity appears along the western edge of the northern Apennines. The synthetic seismicity increases in the Calabrian arc, while it becomes comparatively too intense at the eastern edge of Sicily. The average velocities of the blocks are listed in Table 4 and the epicenters of the synthetic earthquakes are shown in Figure 9.

Table 3

Experiment 3

Block	Prescribed velocities of underlying medium in cm per unit of dimensionless time		Average translational and angular velocities of blocks per unit of dimensionless time		
	V_x	V_y	V_x (cm)	V_y (cm)	ω (10^{-6} rad)
I	0	0	–7.42	5.40	0.65
II	0	0	1.87	4.81	–0.08
III	0	0	0.23	6.00	0.10
IV	1.20	45.60	1.70	38.40	0.42
V	33.30	54.60	20.33	41.19	1.31
VI	33.50	77.30	33.69	67.03	0.40
VII	62.70	65.00	39.19	15.89	–1.05
VIII	69.60	74.10	64.31	68.66	–0.05
IX	0	0	3.68	6.62	0.03
X	0	0	–17.80	59.56	0.05
XI	44.40	63.70	36.04	56.28	0.99

Prescribed velocities of boundary blocks in cm per unit of dimensionless time		
Boundary block	V_x	V_y
BB1–BB3, BB6–BB9	0	0
BB4	69.60	74.10
BB5	–25.00	65.00

4.5. Experiment 5

Purpose: To study how the synthetic seismicity depends on the coupling between the blocks and the underlying medium.

Values of the parameters: With respect to Experiment 4, W is decreased for blocks I, III, V, VII, and XI to 0.005 cm/bar, and for block II to 0.015 cm/bar.

Results: The level of the synthetic seismicity increases slightly along the contraction belt in the north-central Apennines and remains too high at the western edge of Sicily and in the extension belt of the northern Apennines. The average velocities of the blocks are listed in Table 5 and the epicenters of the synthetic earthquakes are shown in Figure 10.

4.6. Experiment 6

Purpose: To decrease the synthetic seismicity along the extension belt in the northern Apennines and at the eastern edge of Sicily, and to increase it along the contraction belt in the north-central Apennines.

Values of the parameters: The following changes have been made with respect to the set of parameters used in Experiment 5: For faults 25–27 (the eastern side of the north-central Apennines) the values of W and W_s are set equal to 0.005 and 0.5 cm/bar,

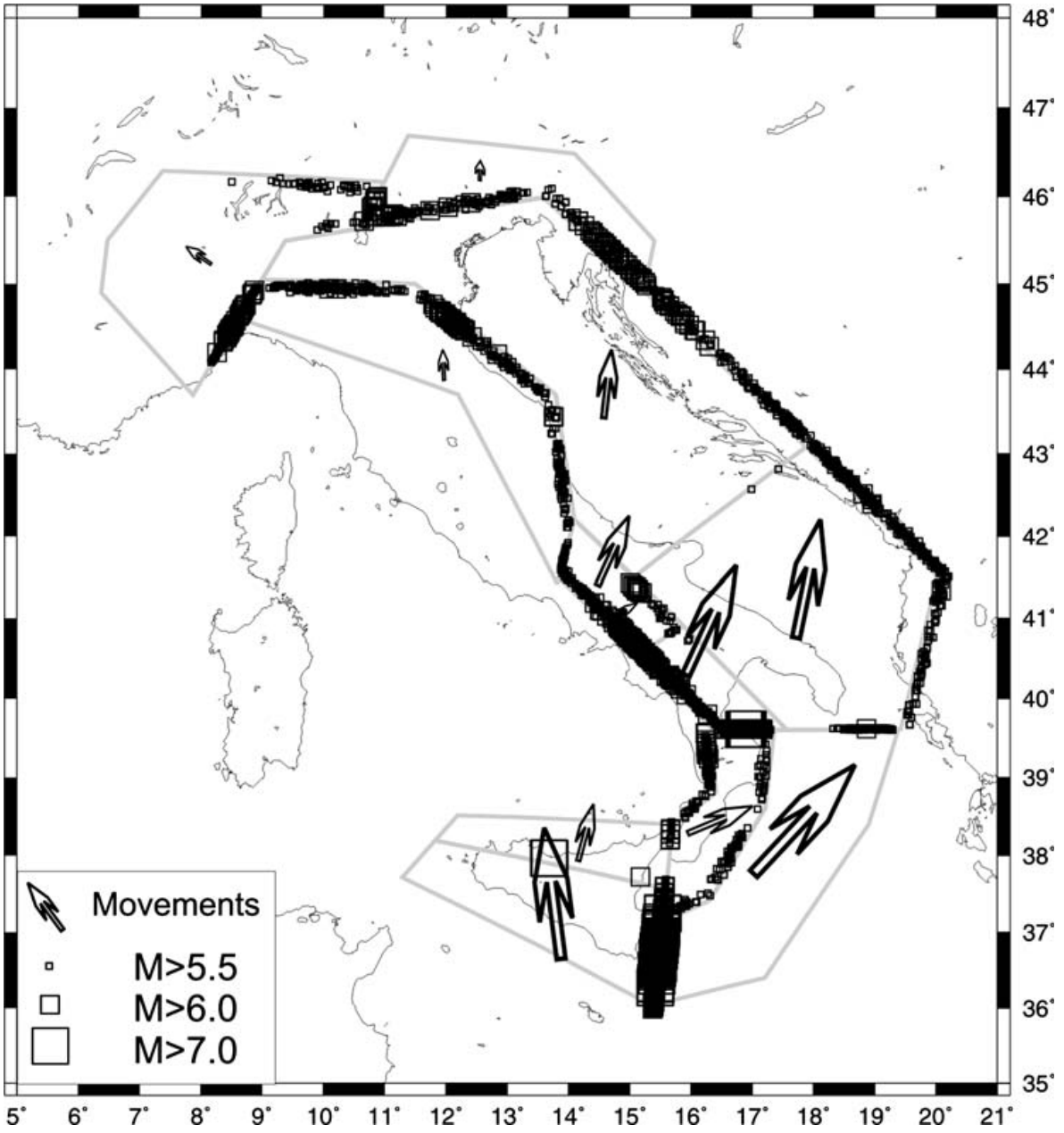

Figure 8
Synthetic seismicity and movements of block structure: Experiment 3.

respectively, and for faults 15, 28, and 29 (the eastern edge of Sicily and the western edge of the northern Apennines) the values of W and W_s are set equal to 0.5 and 50 cm/bar, respectively.

Results: The synthetic seismicity decreases at the western edge of the north-central Apennines and at the eastern edge of Sicily, while it increases in the southern Apennines. The average velocities of the blocks are listed in Table 6 and the epicenters of the synthetic earthquakes are shown in Figure 11.

Table 4

Experiment 4

Block	Prescribed velocities of underlying medium in cm per unit of dimensionless time		Average translational and angular velocities of blocks per unit of dimensionless time		
	V_x	V_y	V_x (cm)	V_y (cm)	ω (10^{-6} rad)
I	0	0	–6.96	5.51	0.62
II	0	0	1.98	4.96	–0.08
III	55.00	45.00	23.06	32.63	–0.30
IV	1.20	45.60	5.38	41.73	0.36
V	33.30	54.60	24.58	41.89	0.98
VI	33.50	77.30	33.85	67.15	0.35
VII	62.70	65.00	38.34	16.28	–1.14
VIII	69.60	74.10	64.25	68.69	–0.05
IX	0	0	–12.82	9.48	0.48
X	0	0	–18.27	59.94	0.07
XI	44.40	63.70	37.09	54.84	1.11

Prescribed velocities of boundary blocks in cm per unit of dimensionless time

Boundary block	V_x	V_y
BB1–BB3, BB6, BB8–BB9	0	0
BB4	69.60	74.10
BB5	–25.00	65.00
BB7	–30.00	30.00

5. Discussion

The experiments described in section 4 aim to reproduce the main features of observed seismicity, by taking into account the basic geodynamic and structural elements of the Italian area. We tested various hypotheses by changing the input parameters of the model. The variation of the velocities of the boundary blocks and of the underlying medium (experiments 1–4) allows us to check the influence of different tectonic forces on the seismicity and on the block kinematics in the study area. The variation of the parameters controlling the rheology of the fault zones and block bottoms (experiments 5 and 6), in agreement with the available information concerning the structural models, permits reproduction of several relevant features of the observed seismicity.

When only the movement of the boundary blocks representing the African plate is specified (Experiment 1), it is impossible to obtain the distribution of the synthetic epicenters and the directions of the block motions like those known from the observations. Decreasing the thickness of the structure (Experiment 2) increases the difference between synthetic and observed seismicity.

In Experiment 3 we assume the existence of an additional factor influencing the overall movement in the region under study: the probable global westward drift of the lithosphere relative to the asthenosphere (or eastward drift of the asthenosphere relative to the lithosphere) as suggested by Doglioni *et al*. (1999b), who showed that the

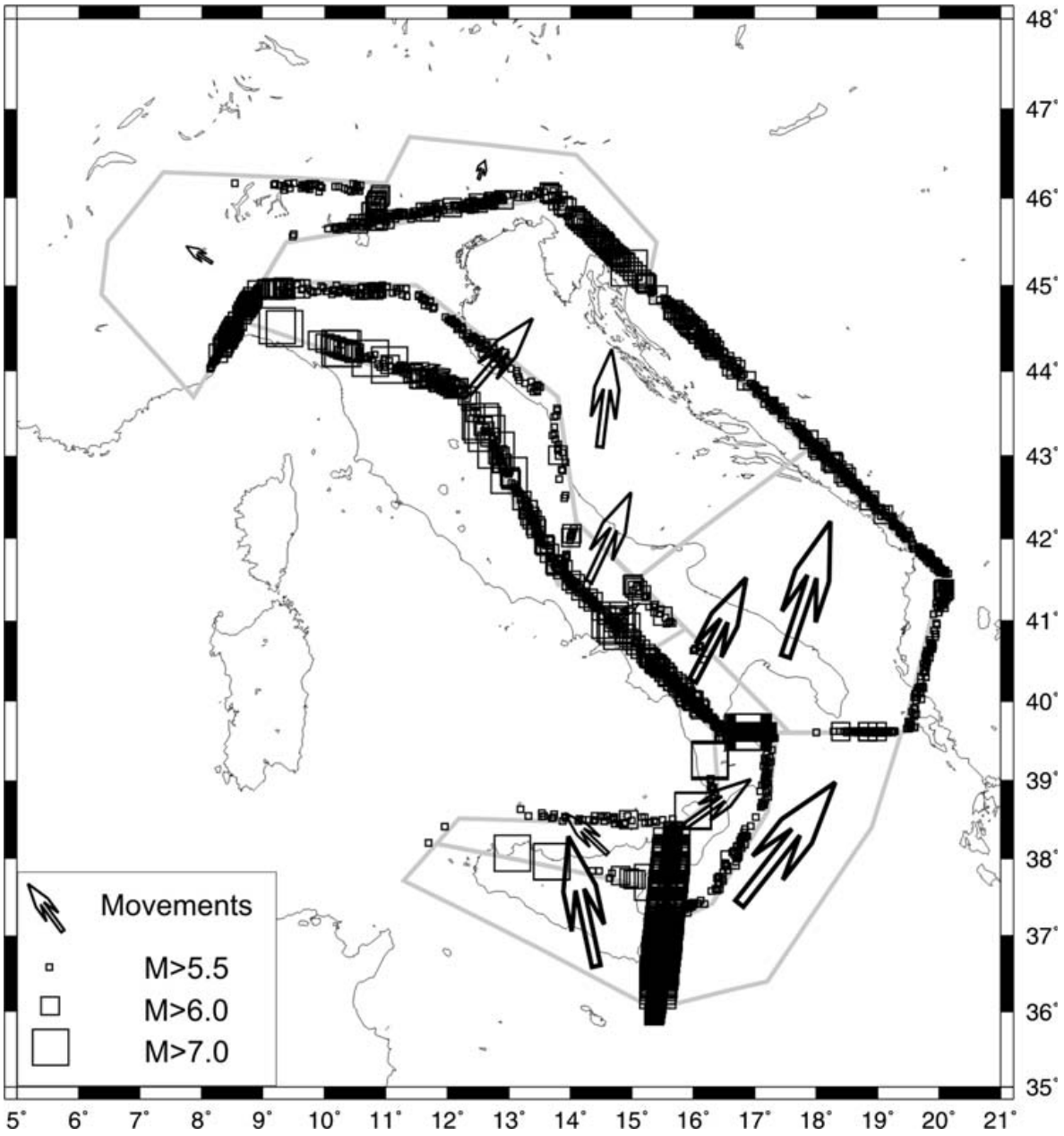

Figure 9
Synthetic seismicity and movements of block structure: Experiment 4.

subduction zones surrounding the Adriatic plate are consistent with the existence of a mantle wedge (PANZA *et al.*, 2003). We introduce the movement of the Adria plate, simulating a rotation around the pole in the Western Alps (MELETTI *et al.*, 2000), with direction in agreement with the configuration of the mantle wedge proposed by DOGLIONI *et al.* (1999b). The resulting movements of the blocks and synthetic seismicity become more similar to the observations than in Experiment 1. This fact can be interpreted as a confirmation that the Adriatic plate is an independent microplate (BATTAGLIA *et al.*, 2004).

Experiment 4 is based on the assumption that the geodynamics of the region is controlled not only by the convergence of Africa and Eurasia, but also by the passive

Table 5

Experiment 5

Block	Prescribed velocities of underlying medium in cm per unit of dimensionless time		Average translational and angular velocities of blocks per unit of dimensionless time		
	V_x	V_y	V_x (cm)	V_y (cm)	ω (10^{-6} rad)
I	0	0	–6.49	5.05	0.58
II	0	0	1.69	4.46	–0.06
III	55.00	45.00	31.92	36.44	–0.56
IV	1.20	45.60	6.20	42.11	0.36
V	33.30	54.60	27.45	43.36	0.87
VI	33.50	77.30	34.03	67.08	0.36
VII	62.70	65.00	46.01	20.00	–0.85
VIII	69.60	74.10	64.79	68.56	–0.04
IX	0	0	–12.80	9.48	0.48
X	0	0	–18.29	59.96	0.07
XI	44.40	63.70	37.85	54.75	1.09

Prescribed velocities of boundary blocks in cm per unit of dimensionless time

Boundary block	V_x	V_y
BB1–BB3, BB6, BB8–BB9	0	0
BB4	69.60	74.10
BB5	–25.00	65.00
BB7	–30.00	30.00

subduction of the south western margin of the Ionian-Adria plate, which causes the opening of the Tyrrhenian basin (e.g., PASQUALE *et al.*, 1997). This speculation is supported by the results of JIMENEZ-MUNT *et al.* (2003) who, by means of an independent method and considering a different scale of investigation, could not obtain a satisfactory result for the geodynamics of the studied area, considering the convergence of Africa and Eurasia only. We model the opening of the Tyrrhenian in its northern part by specifying the movement of the underlying medium for block III (the north-central Apennines) with a velocity in the NE direction that allows us to obtain extension at the western edge of the Apennines and contraction at its eastern edge. One may interpret this as the existence of a rising mantle flow (PASQUALE *et al.*, 1997; SOBOLEV and RUNDQUIST, 1998), which causes the complex structure in the northern Apennines (MELETTI *et al.*, 2000; CHIMERA *et al.*, 2003). This assumption is supported by the high heat flow in the area (DELLA VEDOVA *et al.*, 1991; POLLACK *et al.*, 1993). We model the opening of the Tyrrhenian basin in its southern part by specifying the movement of boundary block BB7 and, as a consequence of this choice, the synthetic seismicity in the Calabrian arc increases. Even if the likelihood of tectonic motions and of synthetic epicenters distribution is improved considerably with respect to previous experiments, the comparative levels of the synthetic seismicity, in the different parts of the structure, are not in sufficient agreement with the observations.

In Experiment 5 we change the visco-elastic characteristics of the block bottoms in Calabria, Apennines and Alps; specifically we decrease the value of W, the growth rate of

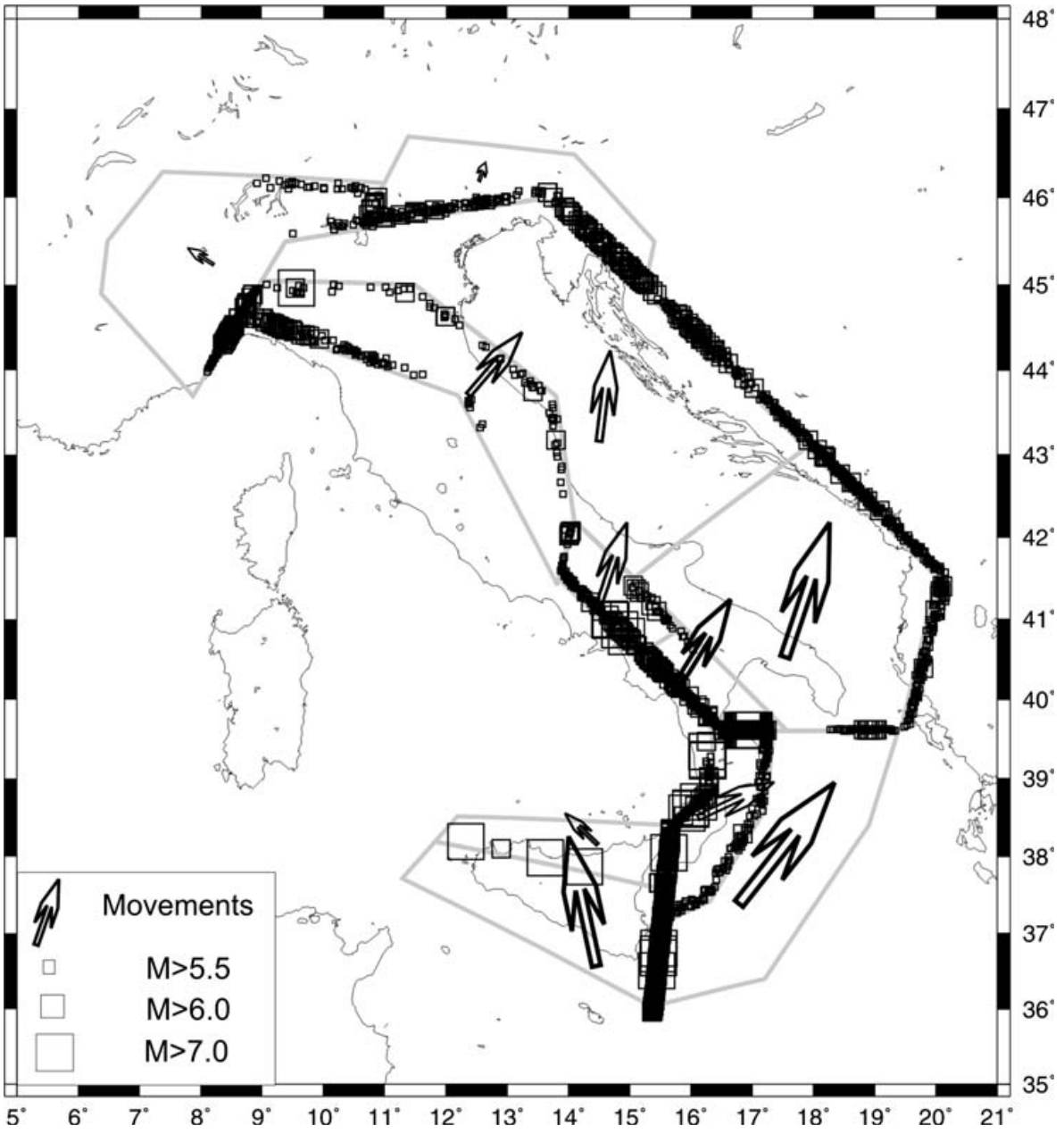

Figure 10
Synthetic seismicity and movements of block structure: Experiment 5.

the inelastic displacements for these block bottoms. This change increases the viscous drag between the block bottoms and the underlying medium and models the coupling along the Apennines, Alps and in Calabria, where lithospheric roots have been evidenced by PANZA *et al*. (2003). With respect to the previous experiments, the increase of coupling increases the transfer from the motion of the underlying medium to the blocks of the structure, and, as a result, the synthetic seismicity raises in the contraction belt of the north-central Apennines and in the southern Apennines.

In Experiment 6 we modify the parameters that define the visco-elastic characteristics of the faults along the eastern edge of Sicily (fault 15 in Fig. 2) and the western edge of

Table 6

Experiment 6

Block	Prescribed velocities of underlying medium in cm per unit of dimensionless time		Average translational and angular velocities of blocks per unit of dimensionless time		
	V_x	V_y	V_x (cm)	V_y (cm)	ω (10^{-6} rad)
I	0	0	–7.09	5.52	0.59
II	0	0	0.65	6.26	–0.03
III	55.00	45.00	46.48	45.24	–0.78
IV	1.20	45.60	6.68	43.91	0.33
V	33.30	54.60	35.43	51.60	0.42
VI	33.50	77.30	36.17	69.78	0.31
VII	62.70	65.00	60.80	24.68	–0.08
VIII	69.60	74.10	68.66	70.85	0.00
IX	0	0	0.06	3.11	0.06
X	0	0	–21.82	63.32	0.03
XI	44.40	63.70	41.13	58.58	1.02

Prescribed velocities of boundary blocks in cm per unit of dimensionless time

Boundary block	V_x	V_y
BB1–BB3, BB6, BB8–BB9	0	0
BB4	69.60	74.10
BB5	–25.00	65.00
BB7	–30.00	30.00

the north-central Apennines (faults 28, 29 in Fig. 2), since the level of the synthetic seismicity obtained along these faults with Experiment 5 is too high. The faults along the eastern edge of Sicily and the western edge of the northern Apennines are located in extensional zones and we assume that the Earth crust here is possibly softer and more plastic than in other parts of the region. This assumption is in accordance with the heat flow data (POLLACK *et al.*, 1993; DELLA VEDOVA *et al.*, 2001) and with the lithospheric S-wave velocities, as reported by PANZA *et al.* (2003) and it allows us to assume that a considerable part of stress is released through creep without earthquakes. We therefore increase the parameters W and W_s that control the increment rate of the inelastic displacements and that may decrease the level of the synthetic seismicity along faults 15, 28, 29. On the contrary, we decrease W and W_s for the faults along the eastern edge of the north-central Apennines (faults 25, 26, 27), as the heat flow is low here (POLLACK *et al.*, 1993; DELLA VEDOVA *et al.*, 2001). As a result the synthetic seismicity in the western edge of the north-central Apennines and in the eastern edge of Sicily decreases.

The sixth variant of the model qualitatively reproduces the basic features of the observed seismicity: Mainly the epicenter distribution and the relative levels of seismicity in different parts of the region, and the overall tectonic motions in the study area. Therefore in the following we analyze quantitatively and discuss in detail the results of Experiment 6.

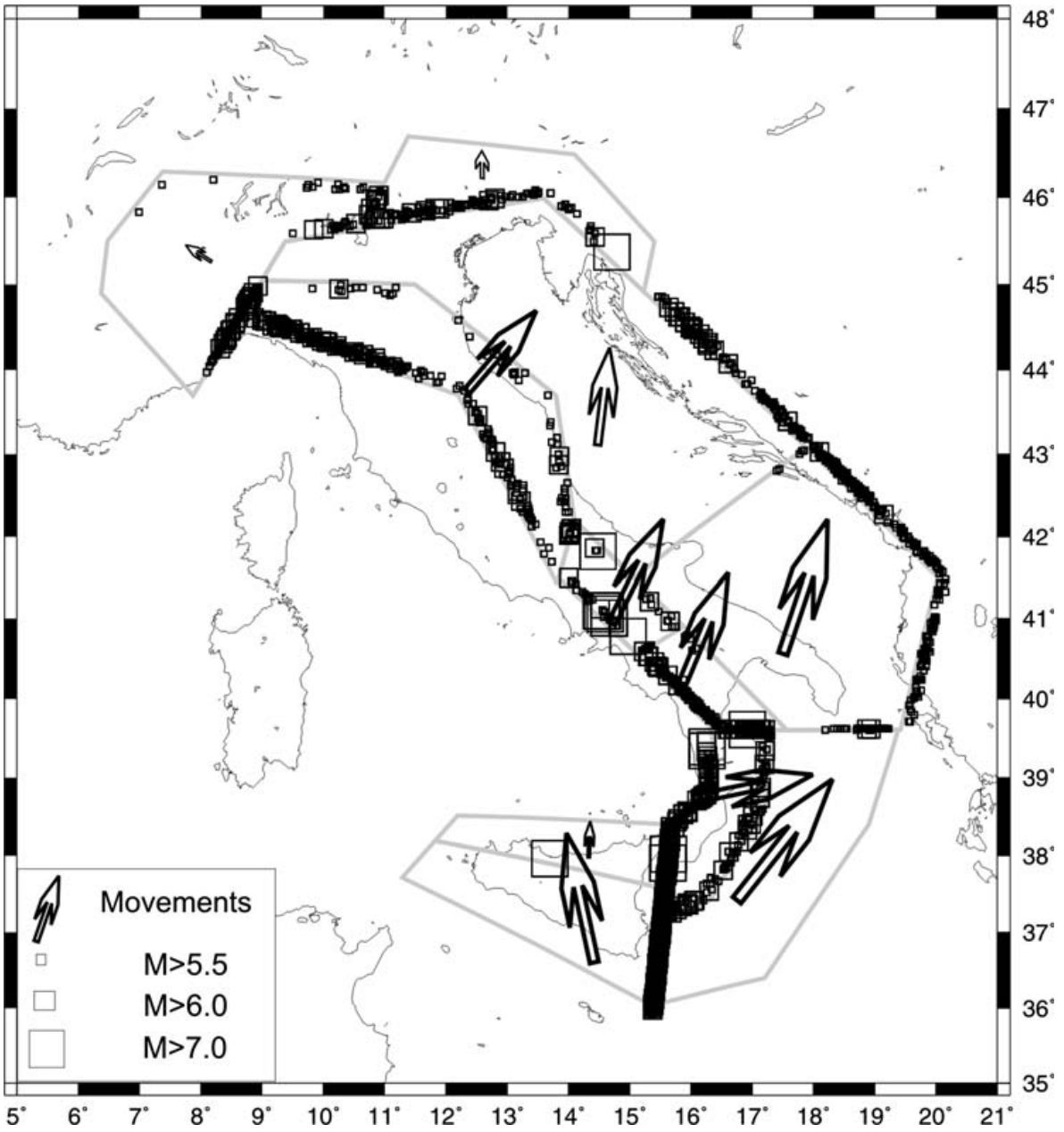

Figure 11
Synthetic seismicity and geometry of block structure: Experiment 6.

5.1. Block Movements

The numerical simulation of the block-structure dynamics has been performed for a period of 20 units of dimensionless time. The resulting average velocities of the blocks are shown in Figure 12 by open arrows, while the black arrows indicate the motion inferred from the geodetic measurements (DEVOTI *et al.*, 2002). Observed movements are available for blocks III, IV, VI, X, XI. The movements obtained in the model exhibit a good agreement with these observations. The values of the average translational and angular velocities of the blocks of the structure are given in Table 6. All blocks move in

the NE direction except blocks I and X which represent the western Alps and Sicily and move in the NW direction. The absolute values of velocities decrease going northward, and blocks I and II, representing the Alps, are almost motionless; this fact is in qualitative agreement with the results of JIMENEZ-MUNT *et al*. (2003) and might be explained, to some extent, by the predominance there of vertical motions (GUBLER *et al*., 1981; GEIGER *et al*., 1986; BROCKMANN *et al*., 2001; CALAIS *et al*., 2000), which cannot be reproduced by the modeling.

The counter clockwise rotation of blocks IV and VI is in good agreement with the rotation of the Adria plate (MELETTI *et al*., 2000). Comparing the resulting velocities of the blocks (Table 6 and Fig. 12) it is possible to observe that there is extension on faults 28, 29 30 and 32 in Figure 2, which represents the extension zone along the Apennines, and compression at the eastern edge of block III, which represents the contraction band along the Adriatic Sea in the north-central Apennines. Contraction zones are formed along the eastern edge of blocks IV and VI (the boundary between Adria and Dinarides), and along the southern boundary of the Alps (fault 24 in Fig. 2); while an extension zone is obtained in the Calabrian Arc (faults 19 and 20 in Fig. 2). These results are in agreement with the stress map of Italy (MONTONE *et al*., 1999) and with the World Stress Map (MUELLER *et al*., 2000).

5.2. Synthetic Seismicity

The magnitudes of the synthetic earthquakes range between 5.2, the minimum magnitude allowed by the specified value of ε (5 km), and 7.6. The distribution of the epicenters of the synthetic earthquakes is shown in Figure 11 and appears in rather good agreement with observed epicenters (Fig. 3).

The information pertaining of the observed events is represented by the available historical data listed by LEYDECKER (1991) for the Dinarides and by the catalog UCI2001 (PERESAN and PANZA, 2002) for Italy and its surroundings. The catalog UCI2001 is complete for magnitude 5 and above during the time interval 1000–2000, while the Leydecker catalog is complete in this range of magnitude only since 1900, nonetheless it is still very useful to identify where large earthquakes occurred during the last 1000 years in the part of the study area not covered by UCI2001.

The slope (*b*-value) of the frequency-magnitude (FM) plot (Fig. 13), or Gutenberg-Richter law, appears larger for the synthetic seismicity (1.44 ± 0.07) than for the observed one (1.14 ± 0.05). To draw the FM plot for the observed seismicity, we consider only the period 1900–2000, as the Leydecker catalog is not complete for magnitude 5 before 1900. From the difference in the number of events with magnitude $M \geq 5$, it is possible to estimate that a dimensionless unit of time corresponds to a time interval an order of magnitude larger than the observed one. The difference in the *b*-values obtained for observed and synthetic seismicity may be explained by the fact that the model does not reproduce with sufficient detail the fault network of the region under consideration. As shown by KEILIS-BOROK *et al*. (1997), when the movements of blocks have a rotation component (as in our case) the increase of the fragmentation of the block

structure causes the decrease of the *b*-value for synthetic seismicity. Therefore, the simplifications used in the model, such as the insufficient representation of the fragmentation of the fault network or the rough mechanism of earthquake occurrence (that does not consider the 3-D structure of the earthquake source) may explain the large *b*-value for synthetic seismicity.

Accordingly to the analysis performed by MOLCHAN *et al.* (1997), the *b*-value calculated for the observed seismicity in northern and central Italy is essentially larger than that in southern Italy (excluding Sicily). The *b*-values calculated for these regions, either considering the synthetic seismicity and the earthquake catalog UCI2001, exhibit a similar difference (i.e., 1.76 ± 0.13 in the north-central part of Italy and $1.33 \pm .0.18$ in southern Italy).

In the *North-Central Apennines* (faults 25, 26, 27, 28, and 29 in Fig. 2) the synthetic seismicity is modeled along two belts. In agreement with the observations the western belt is more active than the eastern one. The largest synthetic events (with $M = 6.8$) occur near the junction between the Apennines and the Alps. Actually, some large events (e.g., the $M = 6.7$ Garfagnana earthquake occurred on September 1920), took place in the north-western part of the Apennines, corresponding to the location of fault 28, although the frequency observed for such events is not as high as that shown in Figure 3.

In the *Southern Apennines* (faults 30 and 32 in Fig. 2) the synthetic seismicity is represented along two belts as well, and the level of the synthetic seismicity is higher than in north-central Apennines, in agreement with the observations. The maximum synthetic magnitude equals 7.6. Here the largest observed earthquakes occurred in 1930 ($M = 7.5$) and 1857 ($M = 7.0$), and several events with $M \geq 6.5$ were reported.

In the *Calabrian arc* (faults 19 and 20 in Fig. 2) the level of the synthetic seismicity is high and the maximum synthetic magnitude is 7.3, approaching the value 7.1 of the largest observed earthquake (Messina earthquake, 1908).

At the *eastern edge of the Adria* (faults 9 and 10 in Fig. 2), in the southern part of the Dinarides, the level of the synthetic seismicity, with a maximum synthetic magnitude 6.8, underestimates the observed seismicity, with maximum magnitude 7.5. The highest synthetic seismicity is obtained in the northern Dinarides, where several synthetic earthquakes with magnitude $M \geq 7.5$ occur, the largest registering $M = 7.6$. The maximum magnitude observed here corresponds to the $M = 7.9$ earthquake which occurred in 1348, in the vicinity of the conjunction of the Alps and the Dinarides.

At the *eastern edge of Sicily* (fault 15 in Fig. 2) the maximum synthetic magnitude is 7.2. The largest observed earthquake, with $M = 7.5$, occurred along the Malta escarpment in 1693; several events with $M \geq 6.5$ have also been reported for this fault zone.

In the *Southern Alps* (fault 24 in Fig. 2) the maximum synthetic magnitude is 6.6, and the largest observed earthquake, $M = 6.8$, occurred in 1222.

5.3. Source Mechanisms

The source mechanisms of the synthetic earthquakes have been analyzed in different parts of the block-model. The mechanism of an earthquake is generally described by

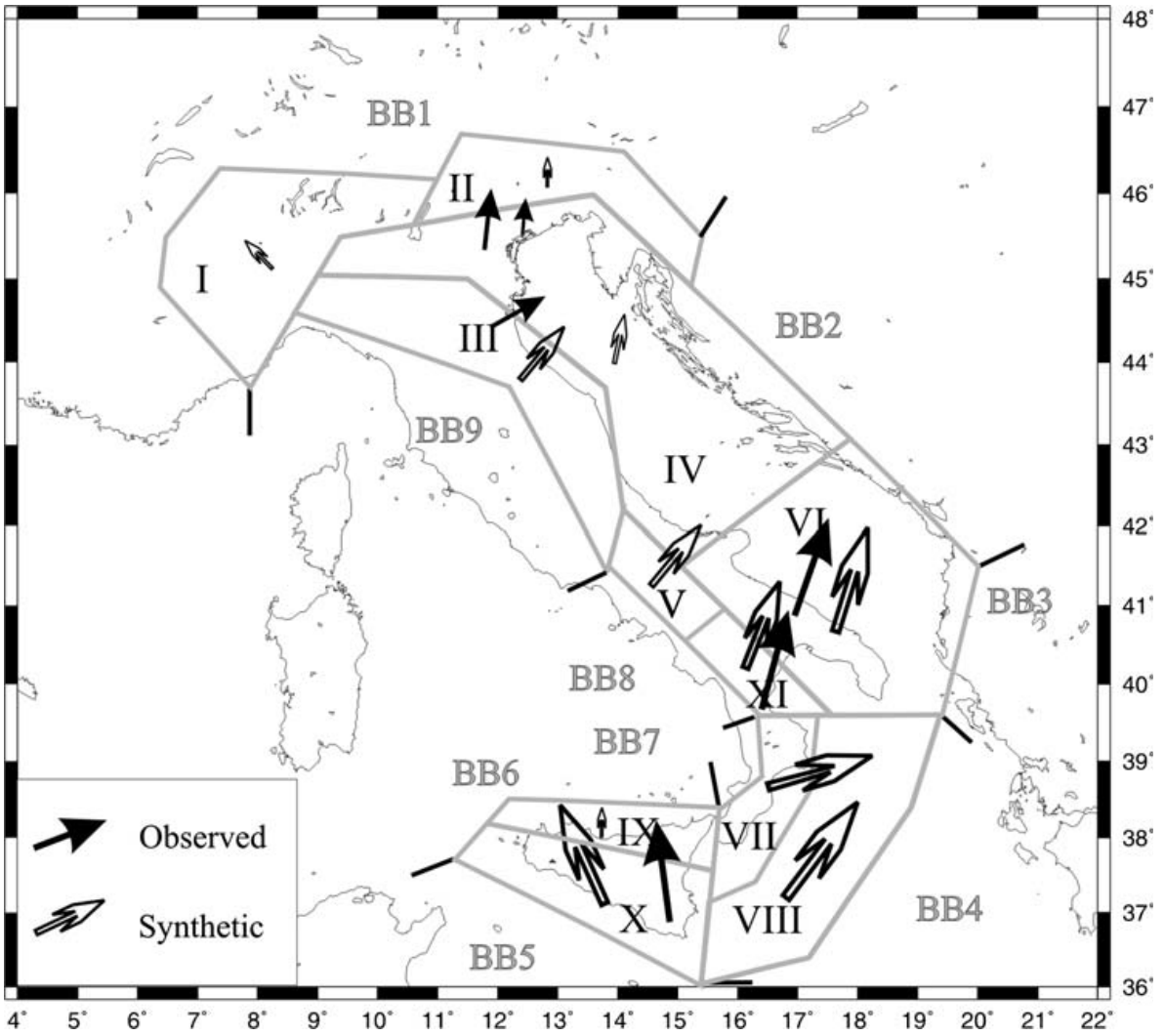

Figure 12
Comparison of the movements (open arrows) obtained in the numerical simulation of experiment 6 with the observations (black arrows) (DEVOTI *et al.*, 2002). The size of symbols is proportional to the values given in Table 6.

means of three angles: strike, dip, and slip (or rake). Strike and dip define the azimuth and the dip angle of the rupture plane, while the slip defines the direction of the displacement along the rupture plane. In the block model, strike and dip are prescribed by the geometry of the block structure; therefore the only free parameter is the slip. The values of slip have the following meaning: 90° and –90° correspond, respectively, to pure reverse and normal faulting, 0° and 180° indicate, respectively, right-lateral or left-lateral pure strike-slip mechanism. Any other mechanism is described by slip values within the above limits.

The available source mechanisms of the observed earthquakes (e.g., SARAÒ *et al.*, 1997; VANNUCCI *et al.*, 2004), shown in Figure 4, are compared with the synthetic ones. We consider several subregions corresponding to different parts of the block structure and the observed fault plane solutions are divided into three groups: strike-slip (rake between –30° and 30°, or –150° and 150°), normal faulting (rake between –30° and –150°), and

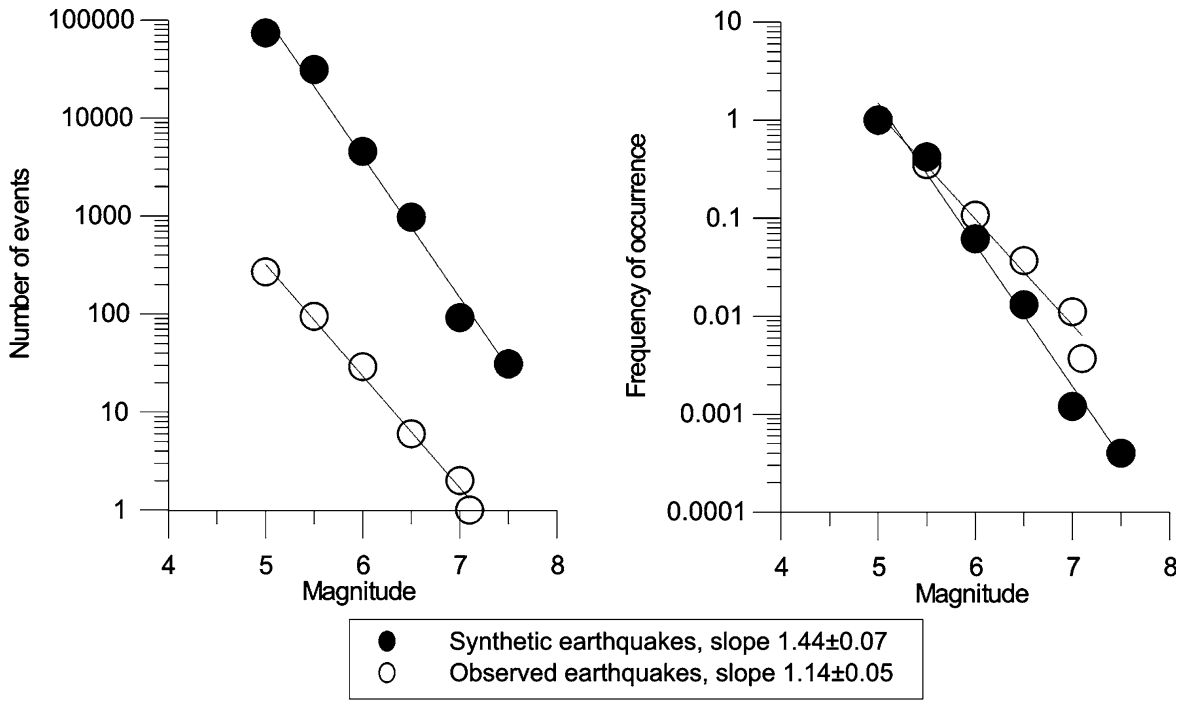

Figure 13
Frequency-magnitude distribution for the synthetic (full circles) and observed (open circles) seismicity.

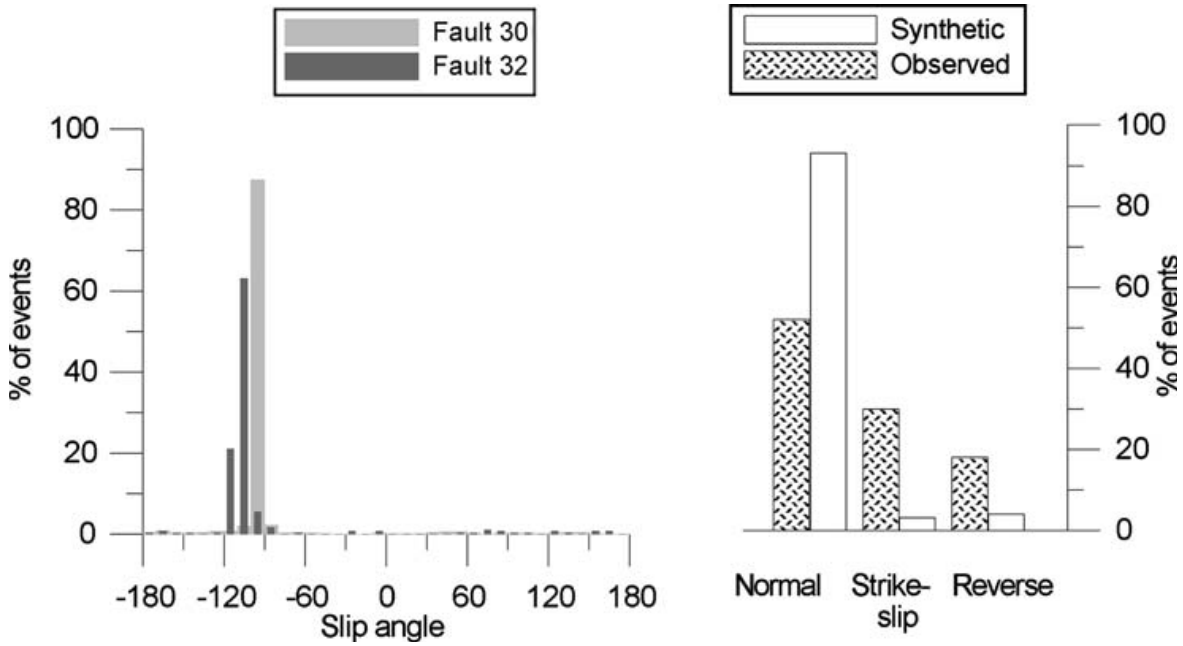

Figure 14
Distribution of the slip angles for the synthetic and observed earthquakes along the north-central Apennines (faults 28, 29 in Fig. 2).

reverse faulting (rake between 30° and 150°). As a whole, the comparison of the mechanisms obtained in the model with the observations and the stress map of Italy (MONTONE *et al.*, 1999) shows a good agreement.

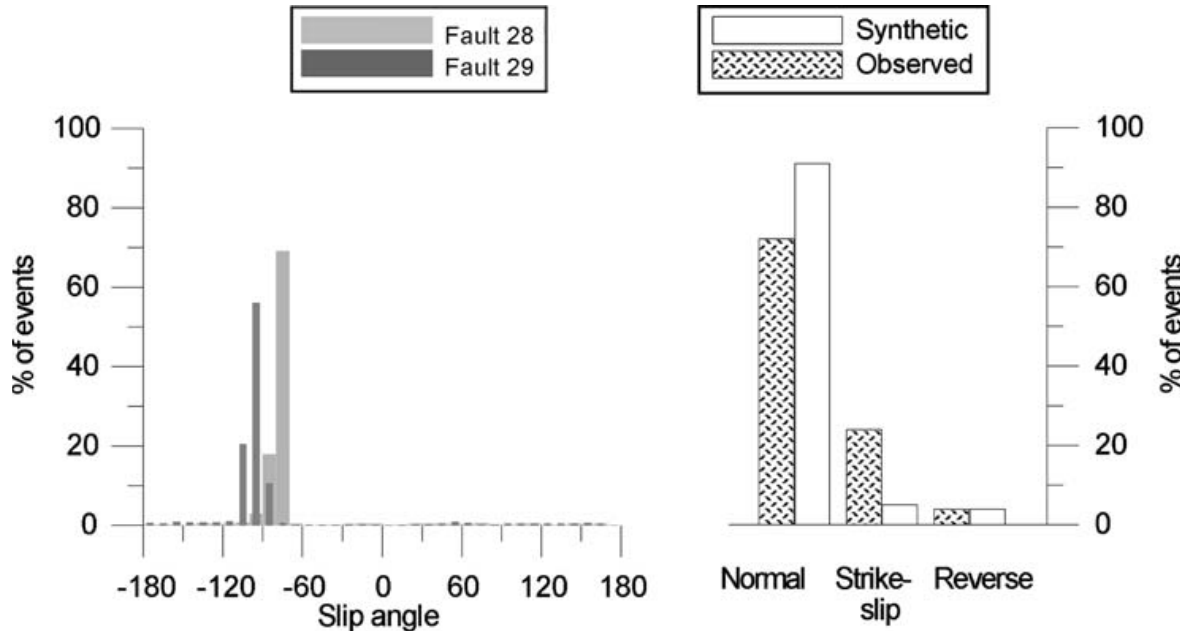

Figure 15
Distribution of the slip angles for the synthetic and observed earthquakes (SARAÒ *et al.*, 1997). along the Southern Apennines (faults 30, 32 in Fig. 2).

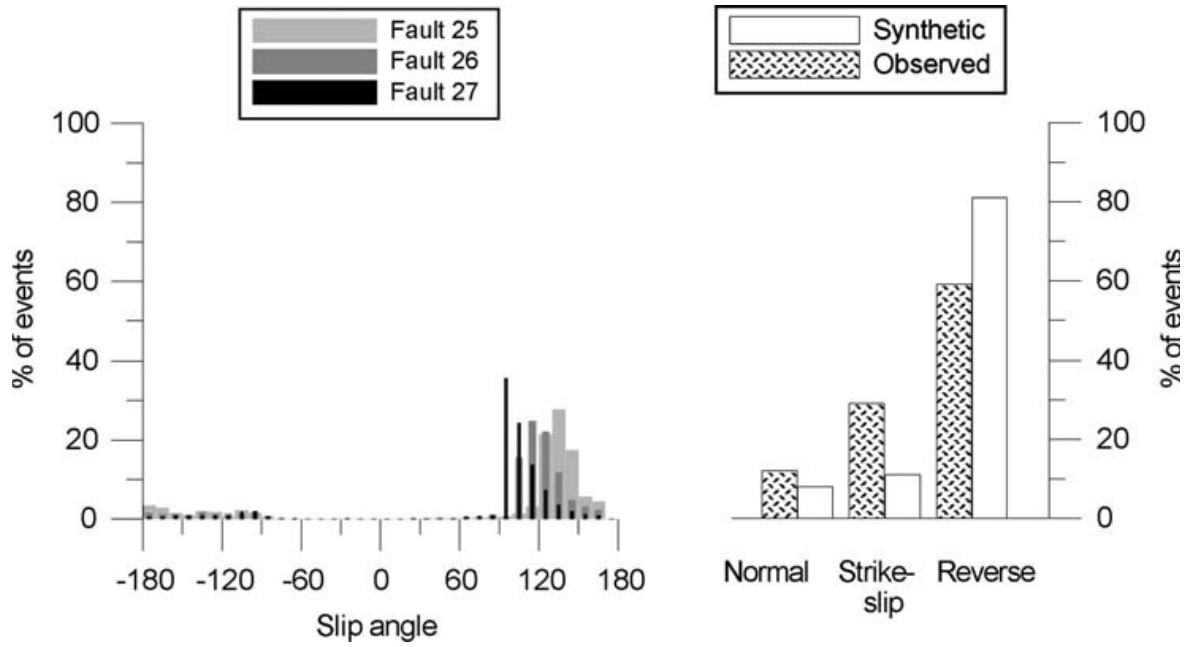

Figure 16
Distribution of the slip angles for the synthetic and observed earthquakes (SARAÒ *et al.*, 1997) along the contraction belt in north-central Apennines (faults 25, 26 and 27 in Fig. 2).

For the north-central Apennines (faults 28, 29 in Fig. 2) and the southern Apennines (faults 30, 32 in Fig. 2) the histograms of the slip values obtained for the synthetic earthquakes are given in Figures 14 and 15. In both histograms the slip varies from –70° to –110°, with a peak near –90°, hence most of the synthetic earthquakes correspond to

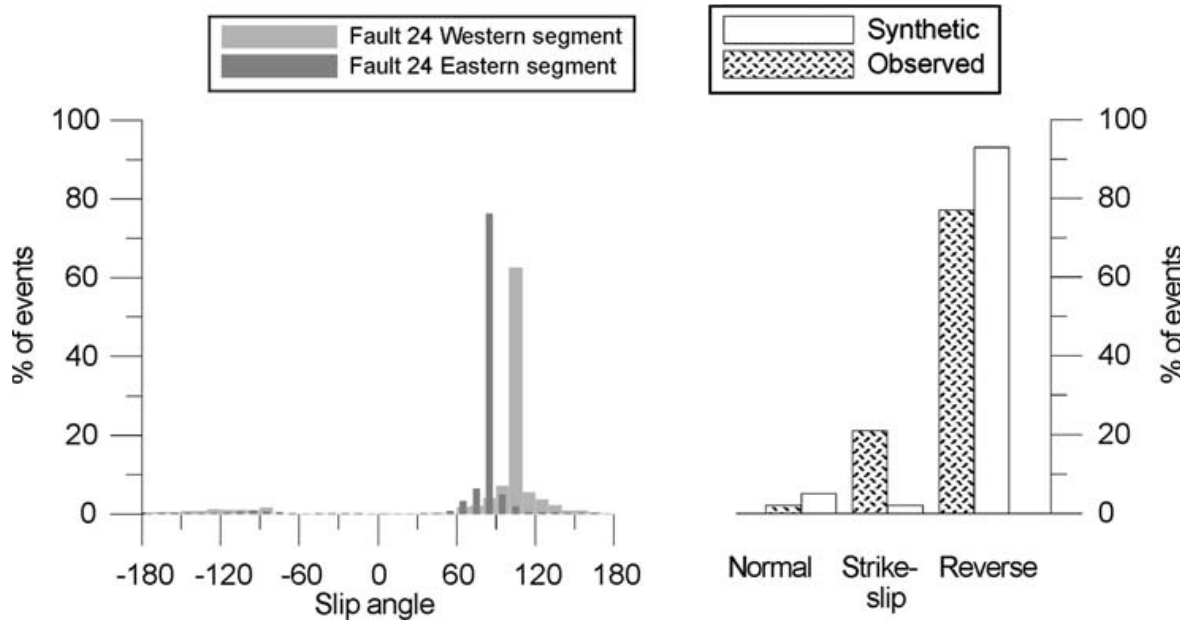

Figure 17
Distribution of the slip angles for the synthetic and observed earthquakes (SARAÒ *et al*., 1997) in the Southern Alps (fault 24 in Fig. 2).

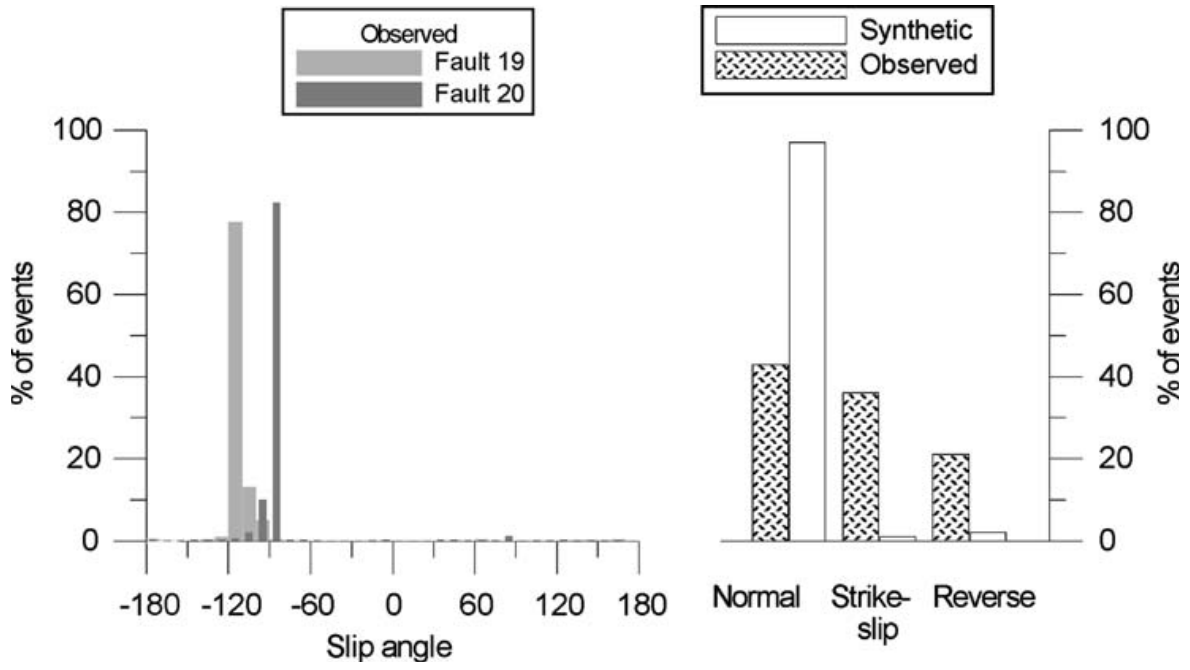

Figure 18
Distribution of the slip angles for the synthetic and observed (SARAÒ *et al*., 1997) earthquakes in the Calabrian arc (faults 19 and 20 in Fig. 2).

normal faulting. The dominating type of observed mechanisms is normal faulting, as can be seen from the percentage of the different observed fault plane solutions, shown in the same figures.

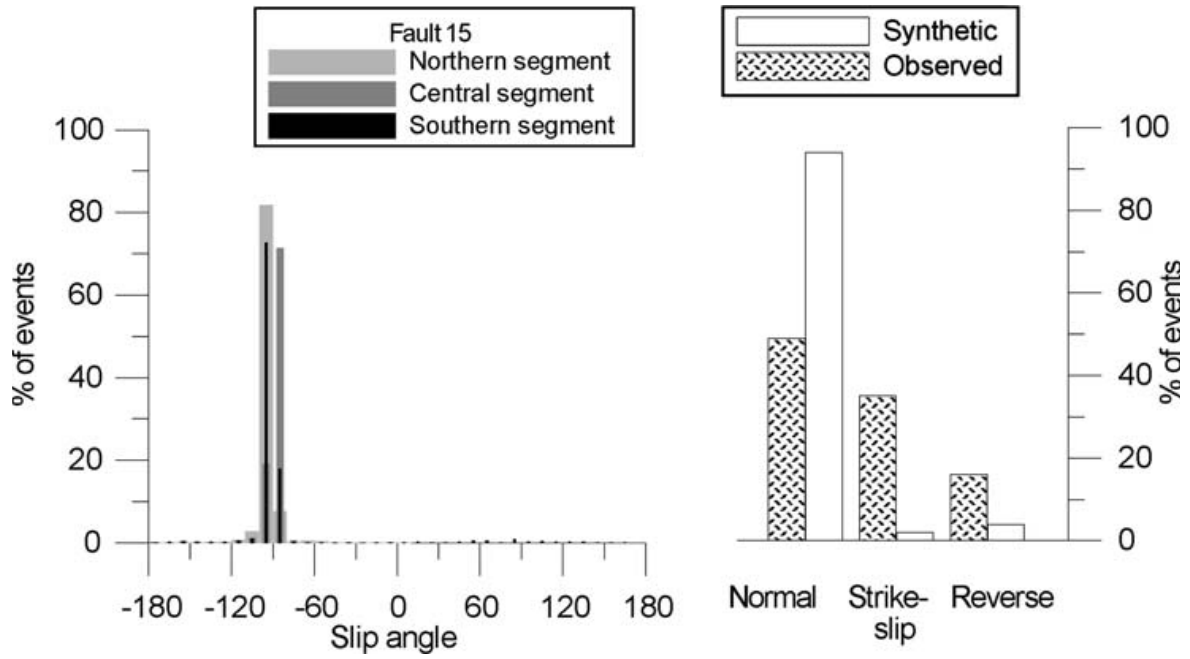

Figure 19
Distribution of the slip angles for the synthetic and observed (SARAÒ *et al*., 1997) earthquakes at the eastern edge of Sicily (fault 15 in Fig. 3).

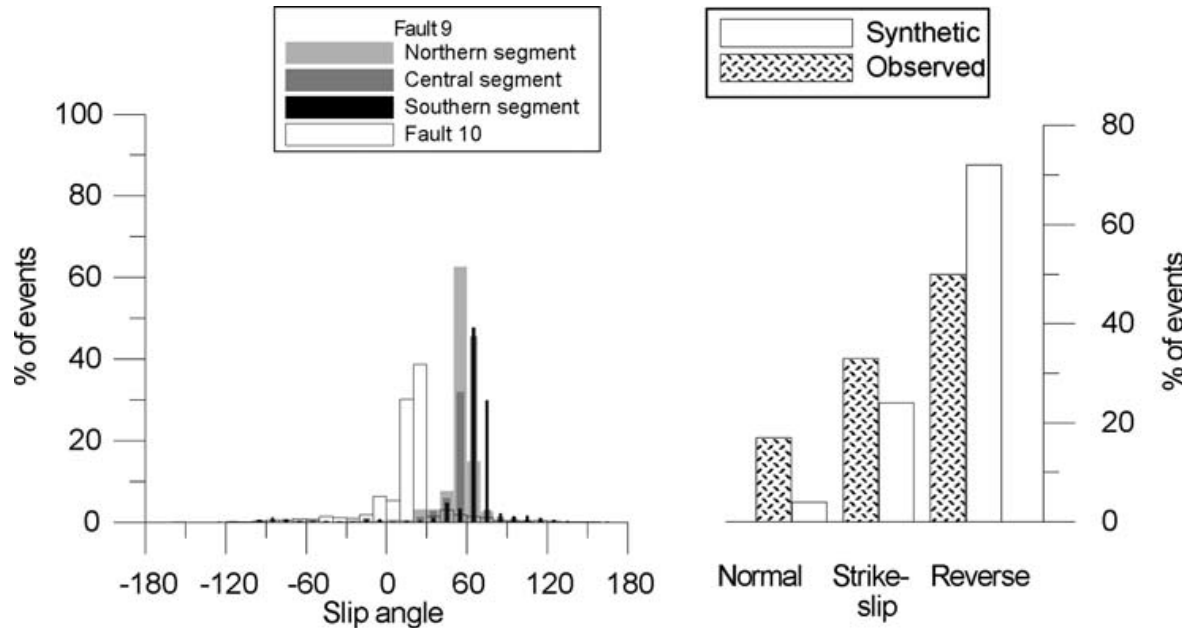

Figure 20
Distribution of the slip angles for the synthetic and observed earthquakes (SARAÒ *et al*., 1997) at the eastern edge of Adria (faults 9 and 10 in Fig. 2).

Similar histograms for the western margin of the Adria plate, along the north-central Apennines (faults 25 and 26 in Fig. 2), are given in Figure 16. Here the histograms maximum is near 120° which corresponds to reverse faulting, but normal faulting and

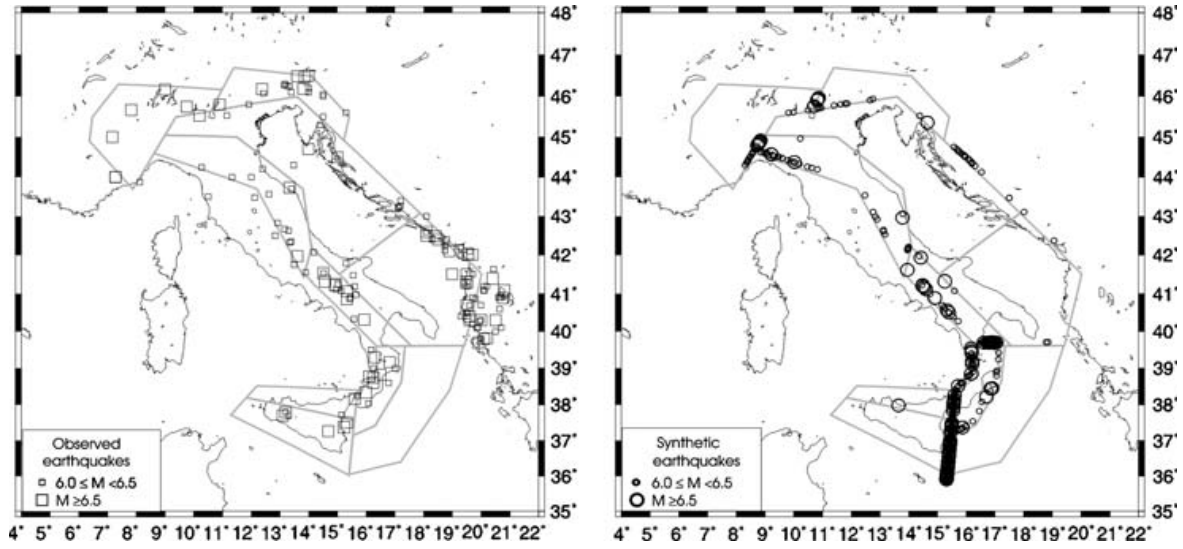

Figure 21
Comparison of the synthetic (Experiment 6) and observed 1000–2000, (PERESAN and PANZA. 2002; LEYDECKER. 1991) seismicity with magnitude $M \geq 6.0$.

strike-slip characterize part of the synthetic earthquakes. The observed fault plane solutions have a similar distribution.

The maximum in the histogram for the southern Alps (fault 24 in Fig. 2) is between 105° and 85° (Fig. 17) which corresponds to reverse faulting, and it complies with the observations.

Most of the synthetic earthquakes obtained for the Calabrian arc (faults 19 and 20 in Fig. 2) show normal faulting, like the observations, and the maximum in the histogram of the slip values is between –80° and –120° (Fig. 18).

The slip values of the synthetic earthquakes obtained for the eastern edge of Sicily (fault 15 in Fig. 2) are concentrated nearby –90° (Fig. 19). Hence, most of the synthetic earthquakes correspond to normal faulting, in fairly good agreement with the distribution of the observed fault plane solutions.

At the eastern edge of the Adria along the Dinarides (fault 9 in Fig. 2) the histogram of the slip values obtained for the synthetic earthquakes peaks between 70° and 50° which corresponds to reverse faulting with a considerable strike-slip component. For the southeastern edge of the Adria (fault 10 in Fig. 2) the slip component increases, and the maximum of the slip histogram is between 30° and 10° (Fig. 20). The observations exhibit a similar behavior.

6. Conclusions

The results of the numerical simulation of lithosphere block-structure dynamics show that it is possible to reproduce the main features of observed seismicity, which are mainly controlled by the motions prescribed in the model. Taking into account rheology, it is

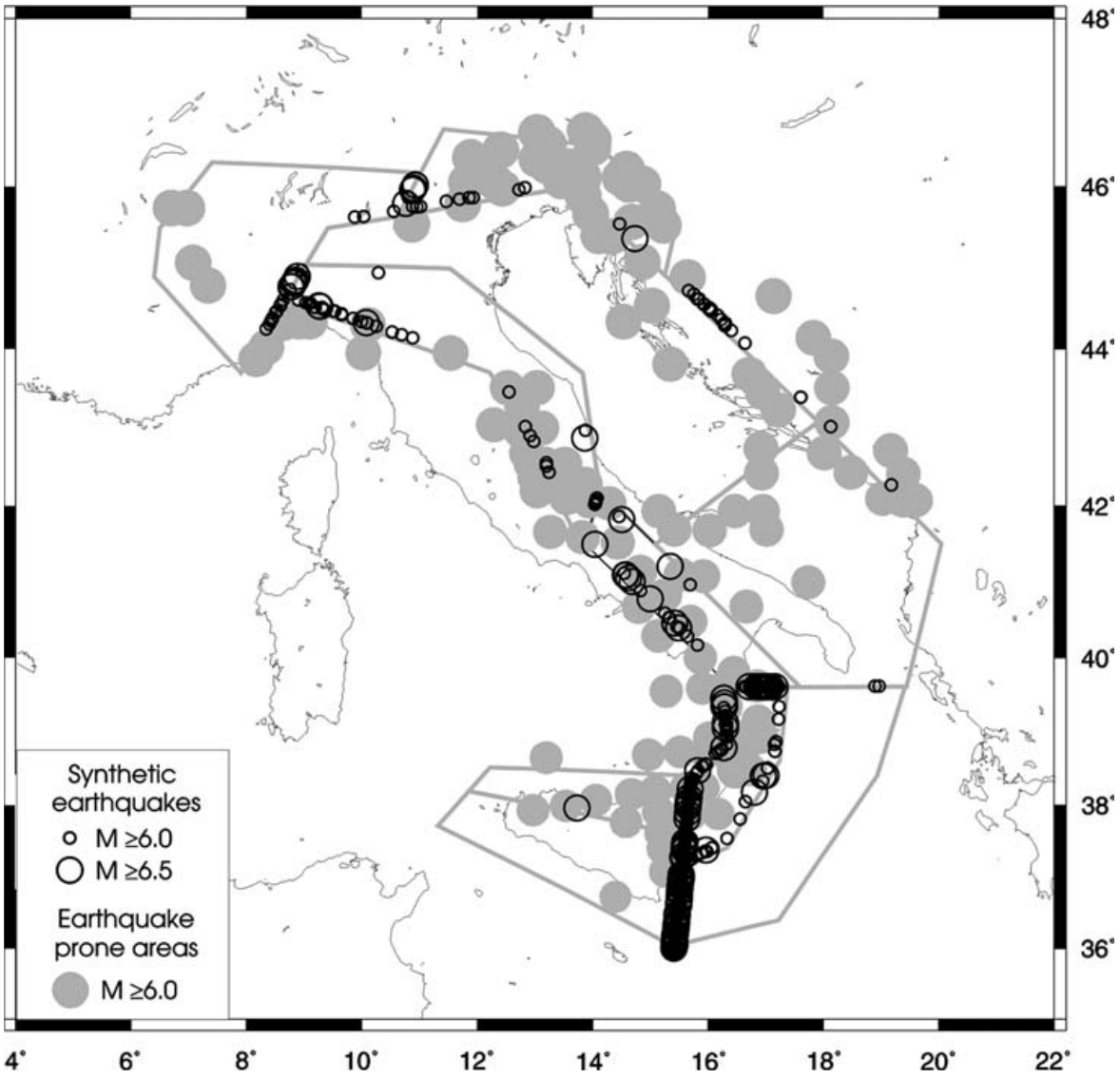

Figure 22
Synthetic earthquakes with M ≥ 6 (Experiment 6) and seismogenic nodes (GORSHKOV *et al.*, 2002).

possible to adjust the relative levels of the seismic activity in the different territories. The distribution of the epicenters of observed and synthetic earthquakes with $M \geq 6.0$ is shown in Figure 21. The best consistency is reached in the belt passing through Sicily, Calabria, and the southern and central Apennines. The largest synthetic events occur along the Malta escarpment, in the Calabrian arc, and in the southern Apennines (to the south of the Ortona-Roccamonfina line); the rate of the synthetic seismic activity in the Apennines decreases from south to north. Nevertheless the level of the synthetic seismicity at the conjunction between the northern Apennines and western Alps is rather high in comparison with the observations, while there is a lack of large synthetic events in the Dinarides, especially in their southern part. Fewer large synthetic earthquakes occur near the conjunction of the Dinarides and the eastern Alps, compared to observations. The synthetic seismicity in the eastern Alps agrees with the observations, while it poorly

correlates with observations in the western Alps. A number of large earthquakes are observed there, while there are no large synthetic events.

The differences between observed and synthetic seismicity possibly can be explained by some of the features of the block-structure geometry. The basis of our block-structure, apart from observed seismicity, is the seismotectonic scheme of SCANDONE *et al*. (1994). The separation of the Adria from the Apennines and the eastern Alps can be easily inferred there, while the boundary between the Po valley and the western Alps cannot be traced unambiguously. Correspondingly, the agreement between synthetic and observed seismicity is good in the Apennines and the eastern Alps and it is poor in the western Alps. The partial disagreement between observed and synthetic seismicity in the Dinarides also may be caused by the incorrect reproduction of the relative movement of block VI and the boundary blocks BB2 and BB3. A revision of the block-structure geometry using as additional information, for example, the morphostructural zoning of the study area (GORSHKOV *et al*., 2002, 2004), and specifying the relevant movements for the boundary blocks BB2 and BB3, may improve the results of the modeling and will be the subject of a forthcoming study.

The comparison of the distribution of the epicenters of synthetic earthquakes with $M \geq 6.0$ with the earthquake-prone areas, determined by GORSHKOV *et al*. (2004) for the same magnitude cut-off (Fig. 22), demonstrates that there is a rather good agreement in the Apennines, in the Malta escarpment and in the Calabrian arc. The agreement is inferior in the Dinarides and there are no synthetic epicenters in the western Alps, where several earthquake-prone areas are identified. The level of the synthetic seismicity is high and the earthquake-prone areas are numerous at the conjunction of the northern Apennines with the western Alps, though no earthquakes with $M \geq 6.0$ have been observed there (see Fig. 21). The correspondence between the results of the modeling of the block-structure dynamics and of the identification of earthquake-prone areas, by the morphostructural zonation, could be an indication for a high seismic potential in this part (conjunction of the northern Apennines with the western Alps) of the study region.

The source mechanisms of the synthetic earthquakes are in a quite good agreement with the available observations (SARAÒ *et al*., 1997; VANNUCCI *et al*., 2004). Normal faulting is typical for the synthetic seismicity in the Apennines, the eastern edge of Sicily and the Calabrian arc, while reverse faulting predominates in the northwestern boundary of the Adriatic Sea, in the southern Alps and along the eastern edge of the Adria along the Dinarides.

The numerical block-model of the lithosphere dynamics for the Italian region permits reproduction of the main observed features of the tectonic motions as well. The movements obtained as a result of the numerical simulation exhibit a good agreement with the available observations (GPS and VLBI); the extension belt along the Apennines and the contraction belt along the northwestern boundary of the Adriatic Sea are reproduced.

The results of the modeling allow us to check some hypotheses regarding the tectonic processes controlling the geodynamics and seismicity in the study area. The main conclusion is that the available observations cannot be explained only as a consequence of

the convergence of Africa and Europe, thus corroborating the results of previous studies, obtained using various geodynamical models. In particular, BASSI and SABADINI (1994) and BASSI *et al*. (1997) showed, by means of a thin-sheet viscous model, that subduction of the Ionian lithosphere underneath the Calabrian arc is necessary to explain the extensional style of the Tyrrhenian Sea, and JIMENEZ-MUNT *et al*. (2003), who used the thin-shell finite-element approach to simulate active deformation in the Mediterranean region, which evidenced that the deformational style in the Mediterranean region is controlled by the Africa-Eurasia convergence and by the subduction in the Calabrian arc and Aegean Sea.

The processes controlling the tectonics and the seismicity in the study region therefore seem to be quite complex. Introducing the rotation of the Adria plate around a rotation pole in the western Alps, we obtain a relatively more credible movement of the block structure, and thus we indirectly support the hypothesis that the Adria is an independent, possibly fragmented (OLDOW *et al*., 2002) microplate, compatible with recent tomographic studies (VENISTI *et al*., 2005). BATTAGLIA *et al*. (2004) reached similar conclusion using GPS measurements and block modeling to study present-day deformations of the Adriatic region. At the same time some additional processes, connected with the passive subduction of the Ionian-Adria plate, seem to play a relevant role in the coexistence of contraction and extension belts in the north-central Apennines (FREPOLI and AMATO, 1997), as well as in the high level of seismicity in the Calabrian arc.

The influence of the geometries and level of detail of the model as well as of the structural properties of the studied region, as reflected by the different coupling of the blocks with the underlying medium and by the differences in the rheology of fault zones, will be the subject of forthcoming investigations.

Acknowledgements

These studies were partly conducted at the Abdus Salam International Centre for Theoretical Physics (Trieste, Italy) within the framework of the SAND group activity. The study was supported by the International Science and Technology Center (project #1538), by NATO (SFP project 972266), by Grant #1269-2003-05 of the President of the Russian Federation for supporting leading scientific schools, and by the James S. McDonnell Foundation within the framework of the 21st Century Collaborative Activity Award for Studying Complex Systems (project *"Understanding and Prediction of Critical Transitions in Complex Systems"*). The study is a contribution to the MIUR-COFINANZIAMENTO (projects 2001, 2002 and 2004) and was partly supported by the Civil Defence of the Friuli Venezia Giulia Region, Italy (DGR 2226 dd. 14.9.2005).

REFERENCES

AIFA, T., FEINBERG, H., and POZZI, J. P. (1988), *Pliocene-Pleistocene evolution of the Tyrrhenian arc: Paleomagnetic determination of uplift and rotational deformation*, Earth and Planet. Sci. Lett. *87*, 438–452.

ANDERSON, H. and JACKSON, J. (1987), *Active tectonics in the Adriatic region*, Geophys. J. R. Astr. Soc. *91*, 937–983.

ANZIDEI, M., BALDI, P., CASULA, G., CRESPI, M., and RIGUZZI, F. (1996), *Repeated GPS surveys across the Ionian Sea: Evidence of crustal deformations*, Geophys. J. Int. *127*, 257–267.

BASSI, G. and SABADINI, R. (1994), *The importance of subduction for the modern stress field in the Tyrrhenian area*, Geophys. Res. Lett. *21*, 329–332.

BASSI, G., SABADINI, R., and REBAÏ, S. (1997), *Modern Tectonic regime in the Tyrrhenian area: Observations and models*, Geophys. J. Int. *129*, 330–346.

BATTAGLIA, M., MURRAY, M., SERPELLONI, E., and BÜRGMANN, R. (2004), *The Adriatic region: An independent microplate within the Africa-Eurasia collision zone*, Geophys. Res. Lett. *31*, L09605, doi:10.1029/2004GL019723.

BENEDETTI, L. (1999), *Sismotectonique de l'Italie et des Regions Adjacentes: Fragmentation du Promontoire Adriatique*, Ph.D. Thesis, Université Paris VII, 354pp.

BROCKMANN, E., GRUNIG, S., SCHNEIDER, D., WIGET, A., and WILD, U., *National report of Switzerland*: Introduction and first applications of a Real Time Precise Positioning Service using the Swiss Permanent Network 'AGNES' In (J.A. and Horni H., Eds.) Subcomission for the European Reference Frame (EUREF). (Dubrovnik, 2001).

BUCK, R., *Consequences of asthenospheric variability on continental rifting*. In Reology and Deformation of the Lithosphere at Continental Margins (eds. Karner, G. D. *et al.*) (Columbia University Press, New York 2003) pp. 1–30.

BURRIDGE, R., and KNOPOFF, L. (1967), *Model and theoretical seismicity*, Bull. Seismol. Soc. Am. *57*, 341–360.

CALAIS, E., BAYER, R., CHERY, F., COTTON, M., FLOUZAT, F., JOUANNE, J., MARTINOD, F., MATHIEU, O., SCOTTI, M., TRADY, C., and VIGNY, C. (2000), *REGAL. A permanent GPS network in The Franch Western Alps*, Configuration and first results. C.R. Acad. Sci. Paris, 331, 435–442.

CALCAGNILE, G. and PANZA, G. F. (1981), *The main characteristics of the lithosphere-asthenosphere system in Italy and surrounding regions*, Pure Appl. Geophys. *119*, 865–879.

CAPUTO, M., PANZA, G. F., and POSTPISCHL, D. (1970), *Deep structure of the Mediterranean basin*, JGREA *75*, 4919.

CAPUTO, M., PANZA, G. F., and POSTPISCHL, D. (1972), *New evidence about the deep structure of the Lipari arc*, Tectonophysics *15*, 219.

CHIMERA, G., AOUDIA, A., SARAÒ, A., and PANZA, G. F. (2003), *Actives tectonics in Central Italy*: Constraints from surface wave tomography and source moment tensor inversion, Phys. Earth Planet. Inter. *138*, 241–262.

CISTERNAS, A., GODEFROY, P., GVISHIANI, A., GORSHKOV, A. I., KOSOBOKOV, V., LAMBERT, M., RANZMAN, E., SALLANTIN, J., SALDANO, H., SOLOVIEV, A., and WEBER, C. (1985), *A dual approach to recognition of earthquake prone areas in the western Alps*, Annales Geophysicae *3*, 249–270.

DELLA VEDOVA, B., MARSON, I., PANZA, G. F., and SUHADOLC, P. (1991), *Upper mantle properties of the Tuscan-Tyrrhenian area: A key for understanding the recent tectonic evolution of the Italian region*, Tectonophysics *195*, 311–318.

DELLA VEDOVA, B., BELLANI, S., PELLIS, G., and SQUARCI, P., *Deep temperatures and surface heat flow distribution*. In Anatomy of an Orogen: The Apennines and Adjacent Mediterranean Basins (eds. Vai, G. B., and Martini, I. P.) (Kluwer Academic Publisher 2001) pp. 65–76.

DEMETS, C., GORDON, R. G., ARGUS, D. F., and STEIN, S. (1990), *Current plate motions*, Geophys. J. Int. *101*, 425–478.

DEMETS, C., GORDON, R. G., ARGUS, D. F., and STEIN, S. (1994), *Effect of recent revisions to the geomagnetic reversal time scale on estimates of current plate motions*, Geophys. Res. Lett. *21*, 2191–2194.

DEVOTI, R. et al. (2002), *Geophysical interpretation of geodetic deformations in the Central Mediterranean area.* In Plate Boundary Zones (eds. Stein, S., and Freymueller, J. T.), Geodynam. Ser., vol. 30, pp. 57–65.

DOGLIONI, C. (1991), *A proposal of kinematic modeling for W-dipping subductions — Posible applicatons to the Tyrrhenian-Apennines system*, Terra Nova *3*, 423–434.

DOGLIONI, C., GUEGUEN, E., HARABAGLIA, P., and MONGELLI, F., *On the origin of west-directed subduction zones and application to the western Mediterranian*. In *The Mediterranean Basins*: *Tertiary Extension within the Alpine Orogen* (eds. Durand, B. *et al.*) (Geological Society, London 1999a) Special Publications, vol. 156, pp. 541–561.

DOGLIONI, C., HARABAGLIA, P., MERLINI, S., MONGELLI, F., PECERILLO, A., and PIROMALLO, C. (1999b), *Orogens and slabs vs. their direction of subduction*, Earth-Sci. Rev. *45*, 167–208.

FREPOLI, A. and AMATO, A. (1997), *Contemporaneous extension and compression in the northern Apennines from earthquake fault-plane solutions*, Geophys. J. Int. *129*, 368–388.

GABRIELOV, A. M., LEVSHINA, T. A., and ROTWAIN, I. M. (1990), *Block model of earthquake sequence*, Phys. Earth Planet. Inter. *61*, 18–28.

GEIGER, A., KAHLE, H-G., and GUBLER, E. (1986), *Recent crustal movements in the Alpine-Mediterranean region analyzed in the Swiss Alps*, Tectonophysics *130*, 289–298.

GIUNCHI, C., KIRATZI, A., SABADINI, R., and LOUVARI, E. (1996), *A numerical model of the Hellenic subduction zone: Active stress field and sea-level changes*, Geophys. Res. Lett. *23*, 2485–2488.

GORSHKOV, A. I., PANZA, G. F., SOLOVIEV, A. A., and AOUDIA, A. (2002), *Morphostructural zonation and preliminary recognition of seismogenic nodes around the Adria margin in peninsular Italy and Sicily*, J. Seismol. Earthq. Engin. *3*, 1–24.

GORSHKOV, A. I., PANZA, G. F., SOLOVIEV, A. A., and AOUDIA, A. (2004), *Identification of seismogenic nodes in the Alps and Dinarides*, Boll. Soc. Geol. It. *123*, 3–18.

GRIPP, A. E. and GORDON, R. G. (1990), *Current plate velocities relative to the hotspots incorporating the NUVEL-1 global plate motion model*, Geophys. Res. Lett. *17*, 1109–1112.

GUBLER, E., KAHLE, H-G., and KLINGELE, E. (1981), *Recent crustal movements in Switzerland and their geophysical interpretation*, Tectonophysics *71*, 125–152.

ISMAIL-ZADEH, A. T., KEILIS-BOROK, V. I., and SOLOVIEV, A. A. (1999), *Numerical modeling of earthquake flow in the southeastern Carpathians (Vrancea): Effect of a sinking slab*, Phys. Earth Planet. Inter. *111*, 267–274.

JACKSON, J., *Velocity fields, faulting and strength on the continents.* In *Reology and Deformation of the Lithosphere at Continental Margins* (eds. Karner, G. D. *et al.*) (Columbia University Press, New York, 2003) pp. 31–45.

JIMENEZ-MUNT, I., SABADINI, R., and GARDI, A. (2003), *Active deformation in the Mediterranean from Gibraltar to Anatolia inferred from numerical modeling and geodetic and seismological data*, J. Geophys. Res. 108 (B1), 1–24.

KARNER, G. D., TAYLOR, B., DRISCOLL, N. W., and KOHLSTEDT, D. L. (eds.), *Rheology and Deformation of the Lithosphere at Continental Margins* (Columbia University Press, New York 2003).

KEILIS-BOROK, V. I., ROTWAIN, I. M., and SOLOVIEV, A. A. (1997), *Numerical modelling of block structure dynamics: Dependence of a synthetic earthquake flow on the structure separateness and boundary movements*, J. Seismol. *1*, 151–160.

KEILIS-BOROK, V. I., and SOLOVIEV, A. A. (eds.) (2003), *Nonlinear Dynamics of the Lithosphere and Earthquake Prediction* (Springer-Verlag, Berlin-Heidelberg).

LEYDECKER, G. (1991), *Historical Earthquake Catalogues: Central and southeastern Europe (342 BC - 1990)*, http://www.bgr.de/quakecat/eng/homepage.htm.

LUNDGREN, P., GIARDINI, D., and RUSSO, R. M. (1998), *A geodynamic framework for eastern Mediterranean kinematics*, Geophys. Res. Lett. *25*, 4007–4010.

MAKSIMOV, V. I. and SOLOVIEV, A. A., *Clustering of earthquakes in a block model of lithosphere dynamics*. In *Computational Seismology and Geodynamics* (ed. Chowdhury, D. K.), vol. 4 (Am. Geophys. Union, Washington, D.C. 1999) pp. 124–126.

MARSON, I., PANZA, G. F., and SUHADOLC, P. (1995), *Crust and upper mantle models along the active Tyrrhenian rim*, Terra Nova *7*, 348–357.

MEIJER, R. T. and WORTEL, J. R. (1996), *Temporal variation in the stress field of the Aegean region*, Geophys. Res. Lett. *23*, 439–442.

MELETTI, C., PATACCA, E., and SCANDONE, P., *Il sistema compressione-distensione in Appennino.* In Cinquanta anni di attività didattica e scientifica del Prof. Felice Ippolito (eds. Bonardi, G. et al.) (Liguori, Napoli 1995) pp. 361–370.

MELETTI, C., PATACCA, E., and SCANDONE, P. (2000), *Construction of a seismotectonic model: The case of Italy*, Pure Appl. Geophys. *157*, 11–35.

MOLCHAN, G., KRONROD, T., and PANZA, G. F. (1997), *Multi-scale seismicity model for seismic risk*, Bull. Seismol. Soc. Am. *87*, 1220–1229.

MONTONE, P., AMATO, A., and PONDRELLI, S. (1999), *Active stress map of Italy*, J. Geophys. Res. *104*, 25595–25610.

MUELLER, B., REINECKER, J., HEIDBACH, O., and FUCHS, K. (2000), *The 2000 release of the World Stress Map*, http://www.world-stress-map.org.

MURRAY, M. and SEGALL, P. (2001), *Modeling broadscale deformation in northern California and Nevada from plate motions and elastic strain accumulation*, Geophys. Res. Lett. *28*, 4315–4318.

NEGREDO, A. M., SABADINI, R., BIANCO, G., and FERNANDEZ, M. (1999), *Three-dimensional modeling of custal motions caused by subduction and continental convergence in the Central Mediterranean*, Geophys. J. Int. *136*, 261–274.

NOCQUET, J. M. and CALAIS, E. (2003), *Crustal velocity field of western Europe from permanent GPS array solutions*, 1996–2001, Geophys. J. Int. 154, 72–88.

OLDOW, J. S., FERRANTI, L., LEWIS, D. S., CAMPBELL, J. K., D'ARGENIO, B., CATALANO, R., PAPPONE, G., CARMIGNANI, L., CONTI, P., and AIKEN, C. L. V. (2002), *Active fragmentation of Adria, the north Africa promontory, central Mediterranean orogen*, Geology *30*, 779–782.

PAMIC, J., BALEN, D., and HERAK, M. (2002), *Origin and geodynamic evolution of Late Paleogene magmatic associations along the Periadriatic-Sava-Vardar magmatic belt*, Geodinamica Acta *15*, 209–231.

PANZA, G. F. (1984), *Structure of the lithosphere-asthenosphere system in the Mediterranean region*, Annales Geophys. *2*, 137–138.

PANZA, G. F., MUELLER, S., CALCAGNILE, G., and KNOPOFF, L. (1982), *Delineation of the north central Italian upper mantle anomaly*, Nature *296*, 238–239.

PANZA, G. F., SOLOVIEV, A. A., and VOROBIEVA, I. A. (1997), *Numerical modeling of block-structure dynamics: Application to the Vrancea region*, Pure Appl. Geophys. *149*, 313–336.

PANZA, G. F., PONTEVIVO, A., CHIMERA, G., RAYKOVA, R., and AOUDIA, A. (2003), *The lithosphere-asthenosphere: Italy and surroundings*, Episodes *26*, 169–174.

PASQUALE, V., VERDOYA, M., CHIOZZI, P., and RANALLI, G. (1997), *Rheology and seismotectonic regime in the northern central Mediterranean*, Tectonophysics *270*, 239–257.

PERESAN, A. and PANZA, G. F. (2002), *UCI2001: The Updated Catalogue of Italy*, ICTP, Trieste, Internal Report, IC/IR/2002/3.

POLLACK, H., HURTER, J., and JOHNSON, R. (1993), *Heat loss from the Earth's interior: Analysis of the global data set*, Rev. Geophys, *31*, 267–280.

PRESS, F. and ALLEN, C. (1995), *Patterns of seismic release in the southern California region*, J. Geophys. Res. *100*, 6421–6430.

SAGNOTTI, L. (1992), *Paleomagnetic evidence for a Pleistocene counterclockwise rotation of the Sant'Arcangelo basin, Southern Italy*, Geophys. Res. Lett. *19*, 135–138.

SAGNOTTI, L., FACENNA, C., and FUNICIELLO, R. (1994), *Paleomagnetic evidence for no tectonic rotation of the Central Italy Tyrrhenian margin since upper Pliocene*, Geophys. Res. Lett. *21*, 481–484.

SARAÒ, A., PANZA, G. F., and SUHADOLC, P., *Waveforms and polarities for exdended and point source studies. Earthquake fault plane solutions: Data bases, derved parameters, geodynamic inferences.* In *Proceedings of the Messina University Forum on "Geodynamics of the Calabrian Arc"* (Taormina, Messina, Italy 1997) pp. 13–17.

SCANDONE, P., PATACCA, E., MELETTI, C., BELLATALLA, M., PERILLI, N., and SANTINI, U. (1990), *Struttura geologica, evoluzione cinematica e schema sismotettonico della penisola italiana*, Atti del Convegno GNDT *1*, 119–135.

SCANDONE, P., PATACCA, E., MELETTI, C., BELLATALLA, M., PERILLI, N., and SANTINI, U. (1994), *Seismotectonic zoning of the Italian peninsula: Revised version*, Working file NOV94.

SCHMID, S. M., PFIFFNER, A., FROITZHEIM, N, SCHONBORN, G., and KISSLING, E. (1996), *Geophysical-geological transect and tectonic evolution of the Swiss-Italian Alps*, Tectonics *15*, 1036–1064.

SOLOVIEV, A. A, VOROBIEVA, I. A., and PANZA, G. F. (1999), *Modelling of block-structure dynamics: Parametric study for Vrancea*, Pure Appl. Geophys. *156*, 395–420.

SOLOVIEV, A. A, VOROBIEVA, I. A., and PANZA, G. F. (2000), *Modelling of block structure dynamics for the Vrancea region: Source mechanisms of the synthetic earthquakes*, Pure Appl. Geophys. *157*, 97–110.

SOLOVIEV, A. and ISMAIL-ZADEH, A., *Models of dynamics of block-and-fault systems*, In *Nonlinear Dynamics of the Lithosphere and Earthquake Prediction* (eds. Keilis-Borok, V. I., and Soloviev, A. A.) (Springer-Verlag, Berlin-Heidelberg 2003) pp. 71–139.

SOBOLEV, P. O. and RUNDQUIST, D. V. (1998), *The relationship between seismicity and geodynamics in the Tethis collision belt*, Doklady Earth Sciences *361*, 700–705.

UTSU, T. and SEKI, A. (1954), *A relation between the area of aftershock region and the energy of main shock*, J. Seismol. Soc. Japan *7*, 233–240.

VANNUCCI, G., PONDRELLI, S., ARGNANI, A., MORELLI, A., GASPERINI, P., and BOSCHI, E. (2004), *An Atlas of Mediterranean Seismicity*, Annales Geophys., Suppl. *47* (1).

VENISTI, N., CALCAGNILE, G., PONTEVIVO, A., and PANZA, G. F. (2005), *Tomographic study of the Adriatic plate*, Pure Appl. Geophys., 162, 311–329.

VOROBIEVA, I. A., GORSHKOV, A. I., and SOLOVIEV, A. A., *Modelling of the block structure dynamics and seismicity for the western Alps*. In *Computational Seismology*, vol. 31 (GEOS, Moscow 2000) pp. 154–169 (in Russian).

WARD, S. N. (1994), *Constraints on the seismotectonics of the Central Mediterranean from Very Long Baseline Interferometry*, Geophys. J. Int. *117*, 441–452.

YAMASHITA, T., and KNOPOFF, L. (1992), *Model for intermediate-term precursory clustering of earthquakes*, J. Geophys. Res. *97*, 19873–19879.

(Received November 1, 2004, accepted June 14, 2007)
Published Online First: November 10, 2007